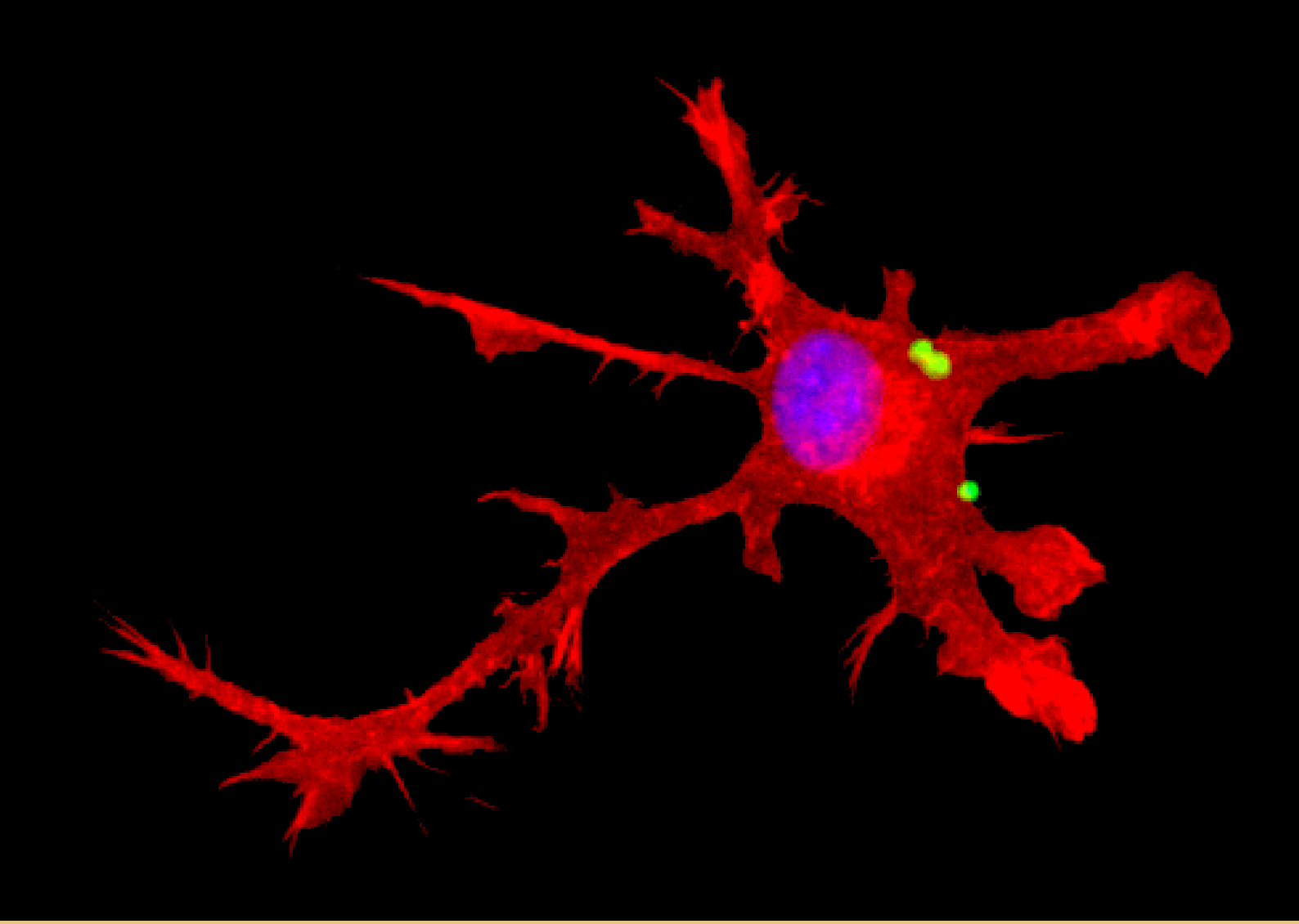

Inês Sofia Dinis Aires

ROLE OF ADENOSINE A_{2A} RECEPTOR IN PRESSURE-INDUCED RETINAL MICROGLIA REACTIVITY

Dissertação para a obtenção do grau de Mestre em Investigação Biomédica sob orientação científica da Doutora Ana Raquel Sarabando Santiago e co-orientação do Doutor António Francisco Rosa Gomes Ambrósio e apresentada à Faculdade de Medicina da Universidade de Coimbra.

Junho de 2014

· U C ·

Universidade de Coimbra

On the front page:

Microglia cell (BV-2) stained with phalloidin (red) with engulfed beads (green), Nuclear staining blue (DAPI).

Role of adenosine A_{2A} receptor in pressure-induced retinal microglia reactivity

Inês Sofia Dinis Aires

Dissertação apresentada à Faculdade de Medicina da Universidade de Coimbra para cumprimento dos requisitos necessários à obtenção do grau de Mestre em Investigação Biomédica. Este trabalho foi realizado no Centro de Oftalmologia e Ciências da Visão, no Instituto de Imagem Biomédica e Ciências da Vida (IBILI) da Faculdade de Medicina da Universidade de Coimbra, sob a orientação científica da Doutora Ana Raquel Sarabando Santiago e supervisão do Doutor António Francisco Rosa Gomes Ambrósio.

Universidade de Coimbra

2014

Este trabalho foi em parte financiado por: Fundação para a Ciência e Tecnologia (FCT) e FEDER. FCT (PTDC/BIM-MEC/0913/2012); FCT projecto estratégico (PEst-C/SAU/LA0001/2013-2014).

"O entusiasmo é a maior força da alma. Conserva-o e nunca te faltará poder para conseguires o que desejas."

Napoleão Bonaparte

Agradecimentos

Esta tese é fruto do esforço e dedicação de várias pessoas que pelo apoio e disponibilidade me transmitiram a força e conhecimentos necessários para a superação de mais esta etapa. Estas palavras são dedicadas a todos os que de uma forma ou de outra contribuíram para o meu sucesso.

Em primeiro lugar gostaria de agradecer à Doutora Raquel Santiago, orientadora desta tese, pela disponibilidade, pela atenção, por todos os ensinamentos e repreensões que me fizeram aprender, integrar e crescer no mundo da ciência. Tenho de reconhecer todo o esforço e apoio prestado, muitas vezes até de madrugada para que "uma das suas meninas" alcançasse o tão desejado objectivo. Foi difícil, ambas sabemos! Muitas tardes de desespero a olhar para retinas KO ou, possivelmente, não KO e, toda uma descoberta que iniciamos juntas no maravilhoso desconhecido mundo dos explantes de ratinho. (ahh! E não pudemos esquecer as tardes de hipóxia momentânea aquando da montagem dos mesmos!)

Gostaria também de agradecer ao Doutor Francisco Ambrósio, co-orientador desta tese por, prontamente, me ter acolhido no seu laboratório e me ter apoiado, integrado e proporcionado todas as condições para a realização desta tese. Acima de tudo agradeço pela confiança que depositou em mim que muito me motivou na conclusão deste trabalho.

Agradeço também à Doutora Carla Marques por me ter ajudado nas dificuldades e angústias que me foram acompanhando ao longo do ano e, por ter sempre tido um conselho e uma palavra amiga para dar no momento certo.

Não posso deixar de agradecer também à Professora Doutora Manuela Grazina por ter autorizado a utilização do Real-Time-PCR e à Maria João pela paciência e por me ter ajudado na obtenção dos resultados.

Gostaria também de agradecer à Joana Vindeirinho que muito me ajudou na técnica de HPLC e ao Francisco Queiróz pelo apoio prestado na quantificação de ATP.

Como não poderia deixar de ser tenho de deixar um obrigado a todos os meus colegas de trabalho à Joana, à Marlene, à Catarina, à Sónia, à Elisa, ao Dan, por me terem ensinado e acompanhado durante este longo percurso.

Gostaria de deixar um especial agradecimento:

À Sandra por termos começado juntas e, desde sempre, me teres motivado e incentivado a ser melhor sendo um grande exemplo de luta e perseverança.

Ao João por todos os "Tá tudo mal! Isso tá tudo contaminado! Tá tudo mal!" sempre com boa disposição a incentivar o aumento da minha confiança no trabalho do dia-a-dia e, também por toda a disponibilidade e companhia para revestimentos de caixas de cultura em fins-de-semana solitários.

À Filipa por todas as palavras de amizade toda a calma e alegria que me transmitiste ao longo dos intensos dias de trabalho. Teria sido mais difícil sem a tua sensatez e tranquilidade.

À Maria por ter sido a minha companheira nas lutas para fechar a nossa velhinha câmara de pressão, por me ter ensinado quando eu ainda nada sabia e, por me ter apoiado ao longo deste ano, sendo a primeira menina do "A2AR team".

À Tânia quero agradecer pela espontaneidade, por me ter aturado a mim e ao Gato no dia-a-dia durante os últimos meses desta etapa, por todas as conversas de fim de tarde, pela companhia e pela amizade.

Ao Gato quero agradecer toda a companhia que me fez durante a escrita desta tese porque sem as tuas travessuras os meus dias teriam sindo mais difíceis.

À Raquel tenho de agradecer toda a disponibilidade, carinho e dedicação que demostraste pelo teu, pelo meu e pelo trabalho de todos no lab, nunca deixaste ninguém desamparado, estando sempre disponível para ajudar e apoiar. Quero agradecer-te toda a ajuda que me deste desde o primeiro momento, ficando até ser noite no lab, discutindo possíveis resultados e problemas bem como procurando lado a lado comigo todas as soluções para as meninas do A2AR team. Obrigada também pelas conversas motivadoras em todos os momentos em que a chorar te disse "não vou conseguir, é impossível", e tu tinhas razão a tese está pronta porque "se os outros conseguem tu também consegues!".

Às amigas de sempre à Rita, à Sara, à Inês, à Carina pela paciência quando não podia encontrar-vos para tomar café porque tinha células à minha espera, por todos os telefonemas e conversas de motivação e desespero, por todas as saídas e jantares que se concretizaram e acabaram sempre com muitos sorrisos, uns pés doridos e farinha aqui e ali. Por serem as amigas de sempre que por mais que o espaço e a falta de tempo afastem, vão estar sempre lá! Obrigado!

Ao Sérgio quero agradecer todo o carinho, toda a paciência e momentos de cumplicidade que me fizeram lembrar que a vida não é só a ciência. Ainda me lembro do dia em que foste comigo ao lab e viste células ao microscópio pela primeira vez, estavas radiante! Foi um orgulho mostrar-te de perto o meu trabalho fazer-te perceber o porquê de passar tantas horas fechada naquele edifício amarelo mal iluminado, a paixão pela ciência é algo que me move e tu percebeste isso aí e a nossa ligação ficou mais forte de dia para dia!

Agradeço aos meus avôs por todo o carinho e preocupação, porque mesmo sem entenderem o que é uma célula fazerem sempre um esforço para me ouvir e apoiar o meu estudo, motivando-me para dar o meu melhor. Agradeço especialmente às minhas avós, à avó Maria porque me criou, me acarinha e apoia incondicionalmente e à minha avó Helena por ser uma estrelinha no céu a iluminar o meu caminho e me acompanhar todos os dias.

Agradeço ao meu maninho por ser o meu melhor amigo, o companheiro de sempre e pelo abraço bem forte na altura certa, quando o meu mundo desaba tu estás sempre lá para me levantar com uma palavra sábia de carinho e tranquilidade. Sei que sou o teu orgulho e tu és o meu exemplo, o meu Pepas, nunca te vou desiludir, quero fazer mais e melhor para ser como tu!

Acima de tudo gostaria de agradecer aos meus pais por me terem proporcionado este momento, por me terem educado, amado e apoiado nas minhas escolhas por mais que fossem difíceis de entender. Por terem sido sempre o meu abrigo e a minha motivação para ser melhor, por serem dois grandes exemplos de humildade, força e perseverança e porque nada seria sem vocês, obrigado!

Contents

Abbreviations

A1R	A1 receptor
A2AR	A2A receptor
A2BR	A2B receptor
A3R	A3 receptor
AC	Adenylyl cyclase
ADA	Adenosine deaminase
ADP	Adenosine diphosphate
AK	Adenosine kinase
AMP	Adenosine monophosphate
AR	Adenosine Receptors
ATP	Adenosine triphosphate
BCA	Bicinchoninic acid
BRB	Blood-retinal barrier
BSA	Bovine Serum Albumin
cAMP	Cyclic adenosine monophosphate
CD11b	Cluster of differentiation molecule 11B
CNS	Central nervous system
CNTs	Concentrative nucleoside transporters
CREB	cAMP responsive element binding protein
CTCF	Corrected total cell fluorescence
CTZ	Cyclothiazide
Cyt-5'-NT	Cytosolic-5'-nucleotidase
DAPI	4',6-diamidino-2-phenylindole
DHE	Dihydroethidium
Dnase I	Deoxyribonuclease I
Ecto-5'NT	Ecto-5'-nucleotidase
EdU	5-ethynyl-2´-deoxyuridine

Abbreviations

EHP	Elevated Hydrostatic Pressure
ELISA	Enzyme-linked immunosorbent assay
ENTs	Equilibrative bi-directional nucleoside transporters
FBS	Fetal bovine serum
G proteins	GTP-binding proteins
GCL	Ganglion cell layer
GFAP	Glial fibrillary acidic protein
Gi/o	Inhibitory G-protein
Gs	Stimulatory G-protein
HBSS	Hank's balanced salt solution
Hcy	Homocysteine
HPLC	High performance liquid chromatography
Iba-1	Ionized calcium-binding adapter molecule 1
iBRB	Inner blood-retinal barrier
IL	Interleukin
INL	Inner nuclear layer
iNOS	Inducible nitric-oxide synthase
IOP	Intraocular pressure
IPL	Inner plexiform layer
KA	Kainate
LPS	Lipopolysaccharide
MAP	Mitogen-activated protein
MEM	Eagle’s minimum essential medium
NFL	Nerve fiber layer
NO	Nitric oxide
oBRB	Outer blood-retinal barrier
ONL	Outer nuclear layer
OPL	Outer plexiform layer

OS/IS	Outer and inner segments
PBS	Phosphate-buffered saline
PFA	Paraformaldehyde
PI3	phosphoinositide 3
PIO	Pressão intra-ocular
PKA	Protein kinase A
PKC	Protein kinase C
RGC	Retinal ganglion cell
ROS	Reactive Oxygen Species
RPE	Retinal pigment epithelium
RPMI	Roswell Park Memorial Institute medium
rTdT	Recombinant Terminal Deoxynucleotidyl Transferase
SAH	S-adenosyl- homocysteine
SDS	Sodium dodecyl sulfate
TE	Tris EDTA
TLR4	Toll-like receptor 4
TLRs	Toll-like receptors
TNF	Tumor necrosis factor
TRIC	Tetramethylrhodamine B isothiocyanate
TUNEL	Terminal deoxynucleotidyl transferase dUTP nick end labeling

Resumo

O glaucoma é uma doença neurodegenerativa caracterizada pela morte das células ganglionares de retina e atrofia do nervo óptico, sendo a segunda principal causa de cegueira a nível mundial. O aumento da pressão intra-ocular (PIO) é o principal fator de risco para o desenvolvimento desta doença. As atuais opções terapêuticas focam-se na diminuição da PIO, mas apesar do controlo da PIO a doença continua a progredir conduzindo à morte das células ganglionares da retina. Assim sendo, novas abordagens terapêuticas devem ser desenvolvidas para proteger as células ganglionares da retina deforma atenuar a progressão da doença. A neuroinflamação parece desempenhar um papel crucial no desenvolvimento da doença. A ativação das células da microglia e o aumento da produção de mediadores pro-inflamatórios foram descritos em modelos experimentais de glaucoma e em doentes, o que pode contribuir para o processo neurodegenerativo.

A adenosina é um neuromodulador do sistema nervoso central exercendo os seus efeitos através de quatro receptores, A_1, A_{2A}, A_{2B}, A_3. O bloqueio dos recetores A_{2A} confere neuroprotecção em diversos modelos de doenças neurodegenerativas como a isquémia cerebral, as doenças de Parkinson, Alzheimer e Huntington. No cérebro, o bloqueio do recetor A_{2A} previne a ativação das células da microglia, e os antagonistas do recetor A_{2A} têm sido propostos como potenciais candidatos para tratamento de doenças neurodegenerativas em que a neuroinflamação está presente.

Neste estudo pretendemos avaliar os efeitos do aumento da pressão hidrostática na reatividade das células da microglia e analisar o efeito do bloqueio dos recetores A_{2A} na prevenção da ativação da microglia desencadeada pelo aumento da pressão hidrostática em culturas primárias de retina, na linha celular de microglia (BV-2) e em culturas organotípicas de retina.

A pressão hidrostática elevada, em culturas primárias de retina, levou a um aumento na produção de espécies reactivas de oxigénio, libertação de citoquinas pro-inflamatórias e morte celular. Além disso, a exposição a pressão elevada desencadeou alterações na morfologia da microglia bem como na sua resposta fagocítica, proliferação e migração, avaliadas nos diferentes modelos celulares.

O bloqueio do recetor A_{2A} diminuiu o stress oxidativo e preveniu as alterações na morfologia, proliferação, migração e fagocitose induzidas pelo aumento da pressão hidrostática.

O aumento da pressão hidrostática conduziu a um aumento dos níveis extracelulares de ATP e de adenosina, o que suporta o papel da adenosina e do receptor A_{2A} na resposta da microglia à exposição à pressão hidrostática aumentada.

Em síntese, os resultados obtidos mostraram que o bloqueio do recetor A_{2A} controlou a ativação da microglia prevenindo a morte das células da retina, o que sugere que os antagonistas dos A_{2A}R podem ter efeitos benéficos no tratamento do glaucoma.

Palavras-chave: Célula da microglia, glaucoma, neuroinflamação, neuroprotecção, pressão hidrostática elevada, recetores A_{2A} de adenosina, retina.

Abstract

Glaucoma is the second leading cause of blindness worldwide being elevated intraocular pressure (IOP) the main risk factor for the onset and progression of the disease. Glaucoma is a neurodegenerative disease characterized by retinal ganglion cell (RGC) loss and optic nerve atrophy. Currently, the therapeutic strategies to treat glaucoma patients are focused on IOP control. However, and despite IOP control, in some patients disease still progresses and patients continue to lose vision. Therefore in addition to lowering IOP, new approaches need to be developed aiming the protection of RGCs. Neuroinflammation may contribute to the onset and progression of glaucomatous disease. Activated microglia have been found in patients and experimental glaucoma models, playing a key role in perpetuating the inflammatory milieu by releasing pro-inflammatory mediators, contributing for the neurodegenerative process.

Adenosine is a neuromodulator in the central nervous system acting through four G coupled receptors, A_1, A_{2A}, A_{2B}, A_3. The blockade of $A_{2A}R$ confers protection in several models of neurodegenerative disorders such as brain ischemia Parkinson's, Alzheimer's and Huntington's diseases. Probably through the control of microglia reactivity. Therefore, $A_{2A}R$ antagonists have been proposed as potential therapeutic options for the treatment of neurodegenerative diseases, in which neuroinflammation plays a role.

In this study we aimed to assess the effects of elevated hydrostatic pressure (EHP) in the reactivity of microglia and to investigate whether $A_{2A}R$ blockade can prevent pressure-induced microglia reactivity in primary retinal neural cell cultures, in a microglial cell line (BV-2) and in organotypic retinal cell cultures.

The exposure of retinal primary mixed neural cell cultures to EHP reactive oxygen species, cytokine release and cell death. Furthermore, EHP elicited changes in microglia morphology, proliferation, migration and phagocytic response, assessed in the different models. The blockade of the $A_{2A}R$ decreased oxidative stress and prevented changes in microglia morphology, proliferation, phagocytosis and migration induced by EHP. The extracellular levels of ATP and adenosine increased upon EHP, supporting a role for adenosine and $A_{2A}R$ activation in the responses of microglia during exposure to EHP.

In summary, our results demonstrated that the blockade of the $A_{2A}R$ was able to control microglia reactivity and afforded protection to retinal cells, suggesting that $A_{2A}R$ antagonists could have beneficial effects for the treatment of glaucoma.

Keywords: Adenosine A_{2A} receptors, elevated hydrostatic pressure, glaucoma, microglial cells, retina neuroinflammation, neuroprotection.

Chapter 1

Introduction

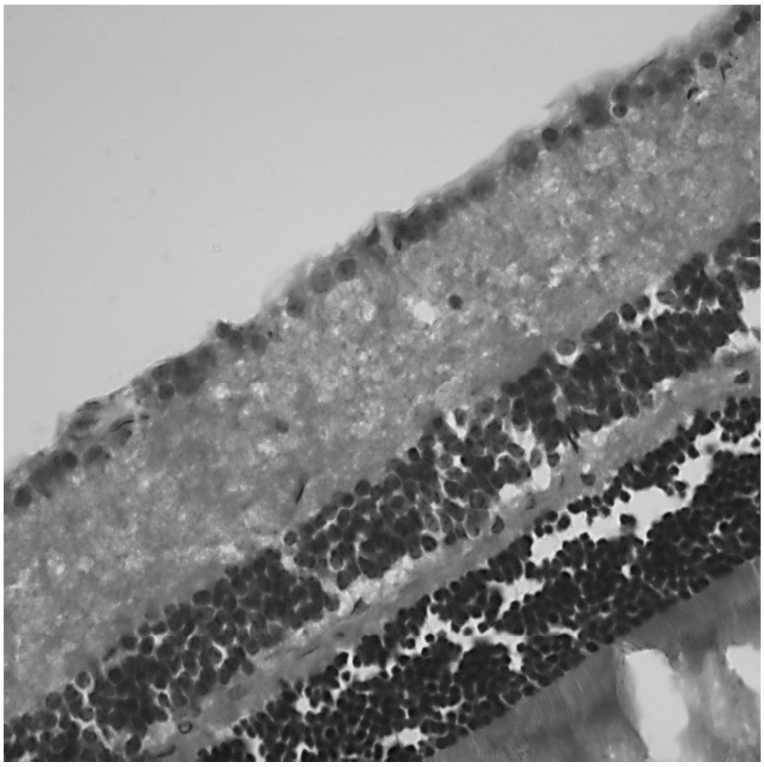

"Retinal section - hematoxylin and eosin staining"

1. Introduction

1.1. Vision

The eyes are the guiders of the mind, allowing each individual to perceive the surroundings opening them a window to the world. In fact, is through the eyes that we acquire information about color, distance and shapes of our environment. In the eye, information conveyed by light is transformed into neuroelectrical signals that are promptly sent to the brain.

1.2. Anatomy of the eye

The eye is a complex optical system that presents us with a view of the surrounding environment. It is organized in order to accomplish two major goals: ensure the normal functioning and maintaining the ideal optical conditions for the access of light to the retina.

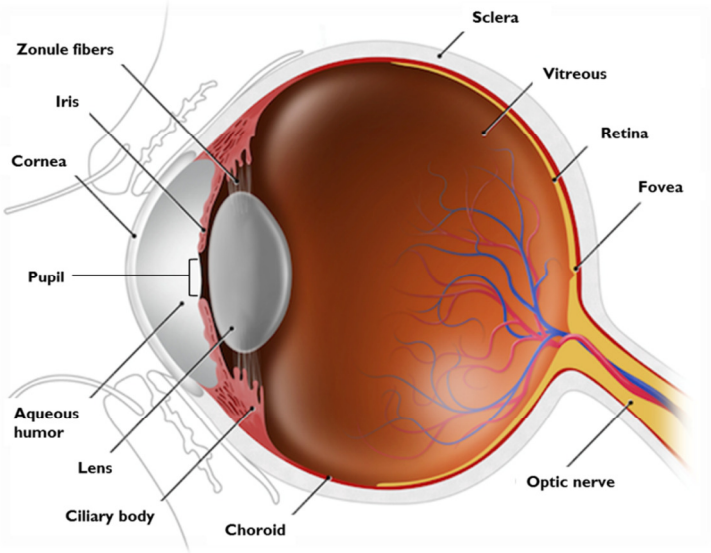

Figure 1 – Anatomy of the human eye (adapted from: http://www.shutterstock.com/).

The eye is constituted by 3 different layers: an external layer, formed by the sclera and cornea; an intermediate layer, distributed into two parts, the anterior (iris and ciliary body) and the posterior (choroid); and an internal layer, or the sensory part of the eye, the retina (Fig. 1). The cornea and the lens are involved in the refraction of light that is

necessary for the formation of focused images on the retina. The sclera is the supportive tissue of the eye conferring structure and protection to the inner tissues. The iris is a thin circular structure in the eye, which contains two sets of muscles with opposite actions functioning as the diaphragm in the cameras, allowing the iris to increase or decrease the pupil's diameter, thus controlling the amount of light reaching the retina. The pigments of the iris confer its color. The function of the ciliary bodies is to determine the refractive power of the lens, allowing the formation of the image through its muscular component and by being attached to it by zonule fibers. The retina is the neuronal tissue of the eye responsible for converting the light impulse into visual signal and conveying it to the brain. The ocular globe is divided in 3 chambers: the anterior chamber located between the cornea and iris, the posterior chamber between the iris and the lens, and the vitreous chamber located between the lens and the retina. The anterior and posterior chambers are filed with aqueous humor that continuously supplies nutrients to the adjacent structures. Aqueous humor is continuously produced by the ciliary processes in the posterior chamber and flow to the anterior chamber through the pupil. The aqueous humor is permanently drained from the anterior chamber through a specialized meshwork of cells situated at the junction of the iris and the cornea (limbus). The vitreous chamber is filled with the vitreous humor, which represents about 80% of the volume of the human eye. The vitreous humor confers shape and structure to the eyeball and it also contains phagocytic cells that remove debris to allow a highly translucent medium to the retina. Adjacent to the retina is the choroid, a highly vascular layer that nourishes the photoreceptors (Purves and Williams, 2004).

1.3. Retina

The retina is the innermost layer of the eye, responsible for converting visual signs into electrical gradients that are transmitted to the brain. Indeed, the retina is part of the central nervous system (CNS), comprising a complex neural circuit constituted by neurons, glial cells and blood vessels. The light must cross all retinal layers to activate photoreceptors. Absorption of photons by the visual pigments of photoreceptors is translated into a biochemical signal, and then into an electrical signal that can stimulate the succeeding neurons of the retina until being transmitted to the brain via the optic nerve (axons of the RGCs).

Besides neuronal cells, the retina is also constituted by glial cells (Müller cells, astrocytes and microglial cells), endothelial cells and pericytes, and epithelial cells. The

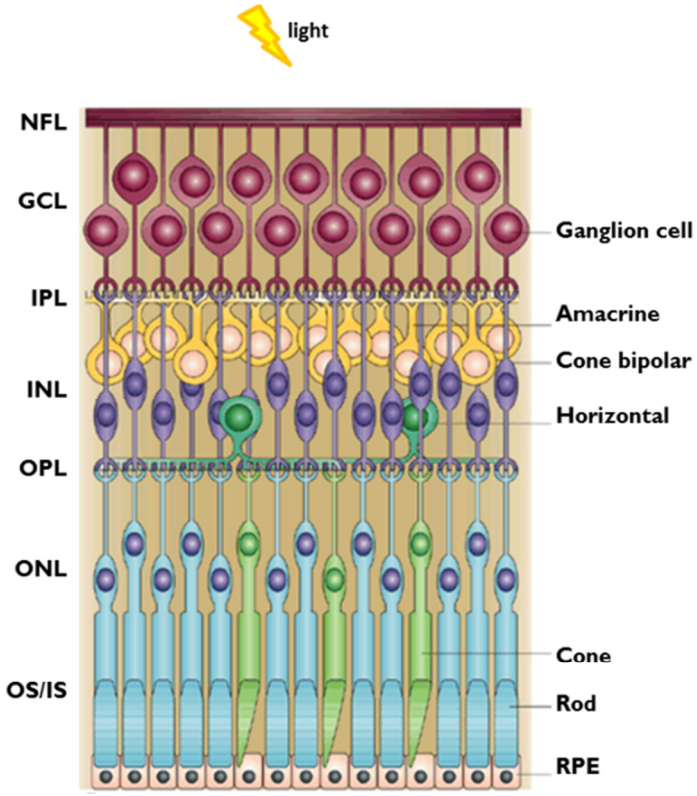

Figure 2 - Retinal structure. Illustration depicting the retinal cell layers and neurons. OS/IS, outer and inner segments of rods and cones; ONL, outer nuclear layer; OPL, outer plexiform layer; INL, inner nuclear layer; IPL, inner plexiform layer; GCL, ganglion cell layer; NFL, optic nerve fiber layer. Adapted from (Kumar, 2001).

retina is highly organized being composed by alternated layers of neuronal cell bodies (nuclear layers) and processes (plexiform layers) (Fig. 2).

The innermost layer adjacent to the vitreous is the nerve fiber layer (NFL) that is formed by the axons of RGCs and is followed by the GCL that contains the cell bodys of RGCs. The inner plexiform layer (IPL) is composed by the axon terminals of bipolar cells that synapse with the RGCs. The inner nuclear layer (INL) contains the nuclei of bipolar, horizontal, amacrine and Müller cells. The outer plexiform layer (OPL) is constituted by the photoreceptor axons and terminal endings that synapse with the dendrites of bipolar and horizontal cells. Immediately adjacent to the OPL is outer nuclear layer (ONL) formed by the nuclei of photoreceptors, followed by the outer and inner segments (OS/IS) of photoreceptors. The outermost layer of the retina is the retinal pigment epithelium (RPE), which is a continuous monolayer of cuboidal epithelial cells (Fig.1) (Kolb et al., 1995; Purves and Williams, 2004).

The RPE is the most important in normal function and support of the outer retina, regulating access of nutrients from the blood as well as in phagocytizing the outer segments of photoreceptors, and in recycling the light-sensitive pigments, essential for the visual cycle (Cunha-Vaz, 2004; Pournaras et al., 2008).

1.3.1. Neurons

The main function of retinal neurons is to convert the light into a neurochemical electrical signal and conveying it into the brain. There are five types of neurons with well-defined functions in the visual pathway (Kolb et al., 1995).

1.3.1.1. Photoreceptors

There are two types of photoreceptors in the retina: rods and cones. Both types have an outer segment composed of membranous disks that contain light-sensitive photopigment and is located next to the RPE, and an inner segment that contains the cell nucleus and gives rise to synaptic terminals that contact bipolar or horizontal cells (Kolb et al., 1995). Rods are responsible for vision at low light since they have sufficient sensitivity to capture the few available photons. On the other hand, cone photoreceptors respond selectively to photons, in normal light, in different regions of the visible spectrum allowing color vision (Wassle, 2004). The two types of photoreceptors are differently distributed across the retina. Absorption of light by the photopigment in photoreceptor outer segments gives rise to a cascade of events, which leads to alterations in the membrane potential and consequently modulates the amount of glutamate neurotransmitter released into the synapse (Kolb et al., 1995).

1.3.1.2. Bipolar cells

Bipolar cells transmit the synaptic input received from photoreceptors to RGCs or amacrine cells. Indeed, signaling from cones and rods is conducted through cone bipolar cells or rod bipolar cells, respectively. The human retina features roughly 10 different types of cone bipolar cells but only one type rod bipolar cells. Furthermore, bipolar cells are involved in the different visual pathways, being their interaction essential in signal modulation and in light adaptation (Kolb et al., 1995).

1.3.1.3. Retinal ganglion cells

Retinal ganglion cells are the neurons responsible for conveying the visual signal originated in the photoreceptors and modulated by bipolar or amacrine cells to the brain. There are two different types of RGCs, the ON and the OFF cell type according to the pathways initiated by bipolar cells (Kolb et al., 1995).

1.3.1.4. Horizontal cells

The human retina has two types of horizontal cells. Both of them feed back onto the rod or cone photoreceptors (Kolb et al., 1995). Horizontal cells modulate signal transmission between photoreceptors and bipolar cells, playing an important role in its receptive field maintaining its sensitivity to light (Kaneda, 2013).

1.3.1.5. Amacrine cells

Amacrine cells modulate the signal transmission between bipolar cells and RGCs at the IPL and help to extract visual elements, such as contrast, color, brightness, and movement. Furthermore, amacrine cells, when excited by synaptic inputs from rod bipolar cells, send excitatory signals to the axon terminals of ON-cone bipolar cells via gap junctions and send inhibitory signals to the axon terminals of OFF-cone bipolar cells through synapses, modulating the signal transmission (Kaneda, 2013).

1.3.2. Visual pathways

The visual pathways can be classified in the horizontal pathway and the vertical pathway. The horizontal pathway, mediated by horizontal cells, modulates the interactions between photoreceptors and bipolar cells at OPL, and amacrine cells at INL, affecting bipolar and RGC communication altering the visual signal. In the vertical pathway, signals from photoreceptors are passed into bipolar cells which synapse directly with RGCs transmitting the signal. In fact, there are two parallel vertical pathways, the cone and the rod pathways. In the cone pathway, cones make direct synapses onto cone bipolar cells which in turn directly synapse with RGCs. This pathway can be further divided at level of bipolar cells being light responses of photoreceptors transmitted into ON- and OFF-pathways. In the mammalian rod pathway, rods make synapses only with rod depolarizing bipolar cell (ON pathway) conveying the signal to the RGCs (Kolb et al., 1995).

1.3.3. Blood vessels

The retina is a tissue with a high metabolism rate needing constant supply of oxygen and nutrients. To fulfil this metabolic request, the retina is supplied by two different sources of blood vessels, the central retinal artery and the choroidal blood vessels. The central retinal artery gives rise to capillaries responsible for nourishing the inner retina, while the choroidal blood vessels provide blood supply to photoreceptors in the outer retina (Klaassen et al., 2013).

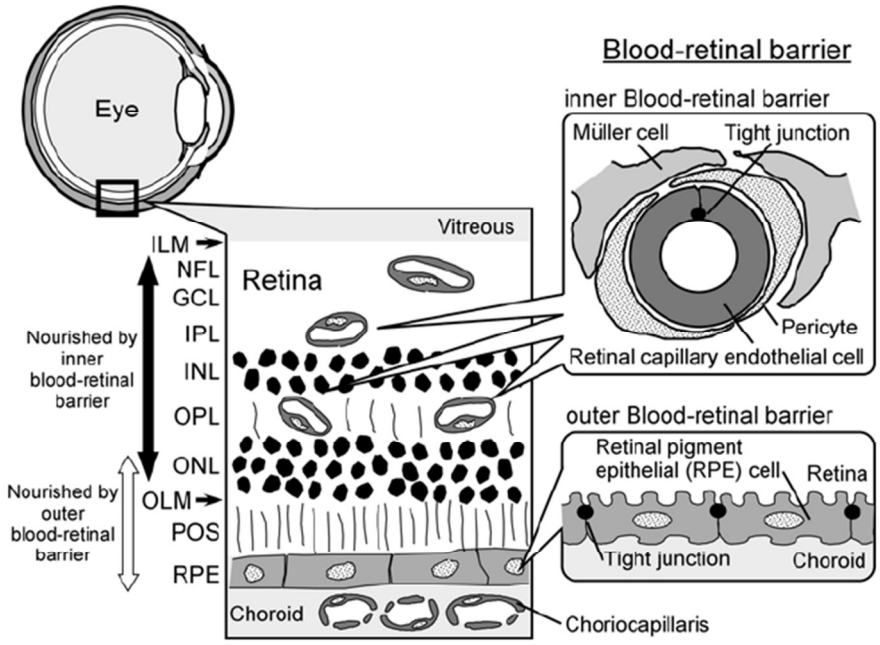

Figure 3 - Illustration of the blood-retinal barrier. RPE, retinal pigment epithelium; POS, photoreceptor outer segments; OLM, outer limiting "membrane"; ONL, outer nuclear layer; OPL, outerplexiform layer; INL, inner nuclear layer; IPL, inner plexiform layer; GCL, ganglion cell layer; NFL, nerve fiber layer; ILM, inner limiting "membrane", from (Hosoya and Tomi, 2008).

In order to allow a suitable, highly regulated, chemical environment for the transparent tissues of the eye, the vascular system is established by two main barrier structures: the blood-aqueous barrier and the blood-retinal barrier (BRB) (Cunha-Vaz et al., 2011). The BRB is formed by highly specialized endothelial or epithelial cells, which restrict the diffusion of molecules by an assembly of proteins that constitutes the functional tight junctions between cells (Leal et al., 2005). Moreover, the BRB can be divided in the inner and outer blood-retinal barriers. The inner blood-retinal barrier (iBRB) is established between tight junctions of endothelial cells and is complemented by astrocytes, Müller cells and pericytes (Fig. 3).

The outer blood-retinal barrier (oBRB) involves three structural entities, the fenestrated endothelium of the choriocapillaris, Bruch's membrane and the RPE. Regarding the importance of the ocular barriers in the regulation of the eye vascular environment, its impairment has already been described to be related to several retinal diseases such as diabetic retinopathy, age-related macular degeneration, retinal vein occlusion, glaucoma and uveitis (Klaassen et al., 2013).

1.3.4. Glial cells of the retina

The retina has three different glial cell types: Müller cells, astrocytes and microglial cells. All glial cells have an important role in maintaining the homeostasis of the retinal tissue (Kolb et al., 1995).

1.3.4.1. Müller cells

Müller cells are the most abundant glial cells in the retina being distributed radially across the thickness of the retina forming architectural support structures. Furthermore, through the extensive ramification of their processes, Müller cells constitute an anatomic and functional link between neurons and blood vessels (Kolb et al., 1995). Müller cells modulate neuronal activity and keep homeostasis by regulating the extracellular concentration of potassium, which is highly increased by light stimulation, and by removing neurotransmitters, such as glutamate, from extracellular space following their release in the synaptic terminal (Newman and Reichenbach, 1996).

1.3.4.2. Astrocytes

Astrocytes are clearly distinguished by the characteristic morphology of a flattened cell body and a fibrous series of radiating processes being almost entirely restricted to the NFL. Astrocytes actively envelope RGC axons forming axonal and vascular glial sheaths, and are connected to blood vessels of the NFL, being part of the BRB. Furthermore, astrocytes also modulate retinal homeostasis by nourishing neurons with glucose and by regulating extracellular potassium levels and metabolism of neurotransmitters (Kolb et al., 1995). In response to noxious stimuli, astrocytes suffer astrogliosis, a process

characterized by changes in morphology, proliferation rate and in the expression of glial fibrillary acidic protein (GFAP) (Hasko et al., 2005).

1.3.4.3. Microglia

Microglia are the immune competent cells of the CNS, seeking for potential threats and responding to alterations of the surrounding environment. Indeed, microglial cells constantly monitor neuronal synapses being able to detect distress signals and remove the impaired neurons having an important role in CNS homeostasis (Wake et al., 2009). Microglial cells originate from monocytic cells that migrated to the CNS during early development from mesodermal/mesenchymal origin (Kettenmann et al., 2011).

In resting state, microglia are ramified and evenly distributed cells. Once they become activated in response to noxious stimuli, such as infection, trauma, ischemia and neurodegenerative disease (Bosco et al., 2011; Hasko et al., 2005), their morphology is altered to a more amoeboid shape with less ramifications (Kreutzberg, 1996; Lee, 2013). Nevertheless, microglia activation cannot be described as a transition from an OFF to an ON state but more like a progressive activation and deactivation state. In fact, a recent study Was focused on this issue, proposing that there are six stages of bidirectional microglial activation and deactivation (Jonas et al., 2012). In the absence of pathological insults, resting microglia are far from dormant being highly dynamic, randomly extending and retracting their processes (Nimmerjahn et al., 2005). In the early phase of neural damage, microglia cells initiate repair mechanisms trying to overcome the injury. Although, excessive or prolonged microglia activation may lead to chronic inflammation with severe pathological consequences that potentially culminate in irreversible neuronal loss. In fact, this deleterious effect of chronic microglia activation has already been described as being related to onset and progression of neurodegenerative diseases such as Alzheimer's and Parkinson's diseases, and also glaucoma (Almasieh et al., 2012; Karlstetter et al., 2010).

Under pathological conditions several mediators are released by injured cells as a distress signal, triggering microglia activation by interaction with immune receptors such as Toll-like receptors (TLRs), scavenger receptors, and numerous cytokine and chemokine receptors (Kierdorf and Prinz, 2013). Furthermore, once activated, microglial cells are able to produce and release pro-inflammatory mediators such as nitric oxide (NO), reactive oxygen species (ROS), cytokines such as tumor necrosis factor (TNF),

interleukin (IL)-1β, and IL-6 (Lee, 2013). Moreover, microglia release chemokines to attract other immune cells and secrete several polypeptide neurotrophic factors, which influence the physiology and survival of surrounding neurons (Kettenmann et al., 2011; Langmann, 2007). Additionally, microglia migrate through the tissue toward lesion areas following chemotactic distress signals (Davalos et al., 2005), and once in lesion site, microglial cells can proliferate (Gomez-Nicola et al., 2013) and dynamically clear their surroundings by phagocytizing debris and apoptotic cells (Petersen and Dailey, 2004).

1.3.4.3.1. Retinal microglia

In the retina, under physiological conditions microglia can be found in the NFL, GCL as well as within IPL or above the INL (Bosco et al., 2011). In resting states microglia are known to release mediators that stimulate the survival and regeneration of RGC and regulate the survival of photoreceptors (Langmann, 2007).

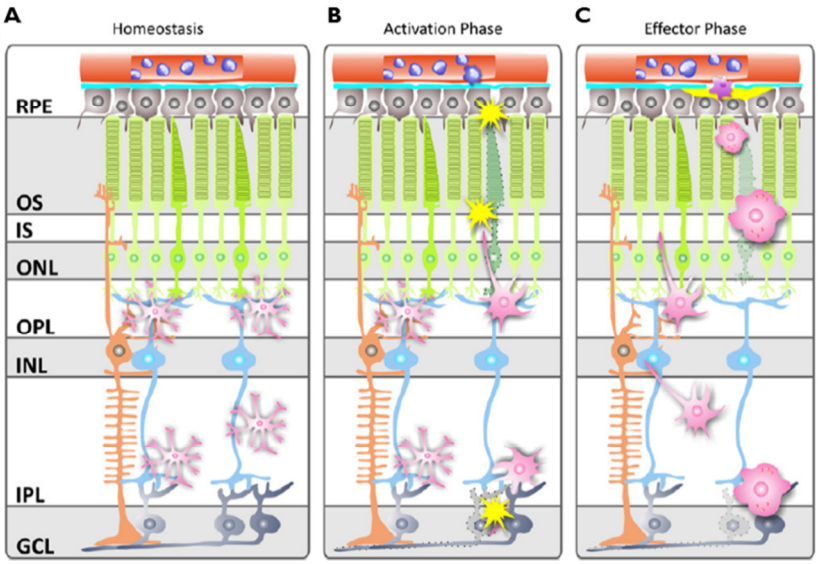

Figure 4 - Schematic representation of three common phases of microglial activity in the retina. (A) In physiological conditions microglia mainly populate the plexiform layers of the retina, continuously scannig their environment, phagocytosing cell debris and secreting neurotrophins; (B) Various noxious stimuli that lead to abnormal cell functions rapidly alert microglia; (C) Microglia quickly migrate to the lesion site, where they transform into amoeboid full-blown phagocytes. RPE, retinal pigment epithelium; ONL, outer nuclear layer; OPL, outer plexiform layer; INL, inner nuclear layer; IPL, inner plexiform layer; GCL, ganglion cell layer (Karlstetter et al., 2010).

Similar to what has been described for brain resident microglia, retinal microglia present alterations in active/resting state and are also involved in retinal

neurodegenerative pathologies such as glaucoma, diabetic retinopathy and age-related macular degeneration (Gupta et al., 2003; Rungger-Brandle et al., 2000; Zeng et al., 2000).

The presence of microglial cells in the vicinity of GCL and IPL suggests that its activation may be implicated in RGC impairment in retinal degenerative diseases. In resting state, microglia present long protrusions that continuously scan retinal parenchyma, phagocytize cell debris and secrete supporting factors (Fig. 4A). Noxious stimuli that lead to abnormal cell function or degeneration, trigger microglia activation (Fig. 4B), promoting cell migration to the lesion site, where they change into amoeboid full-blown phagocytes (Fig. 4C) (Karlstetter et al., 2010). These activated cells may have protective or deleterious effects depending on their immunological phenotype and the local cytokine milieu, as described for brain microglial cells. Recent studies reveal that microglia activation occurs in an early stage of retinal disease suggesting an inductive role of microglia response to disease progression (Lee et al., 2008). Nevertheless, the mechanisms underlying RGC death mediated by microglia activation in neurodegenerative diseases, such as glaucoma, are not yet fully understood.

1.4. Glaucoma

Glaucoma is a group of diseases characterized by progressive optic nerve atrophy and RGC death (Vohra et al., 2013). It is the second leading cause of irreversible blindness worldwide and it is expected that by the year 2020 approximately 80 million people will suffer from this disease (Quigley and Broman, 2006). Furthermore, changes in the visual field are not detected until the disease is advanced, compromising its early diagnostic. Visual loss in glaucoma starts at the periphery, not affecting central vision at first (Cohen and Pasquale, 2014). Elevated intraocular pressure (IOP) is the main risk factor for the development of glaucoma. Nevertheless, patients may present IOP within the normal range and still develop glaucoma. Advanced age has also been identified as an important risk factor for the development of glaucomatous disease (Almasieh et al., 2012; Zhang et al., 2007). Several hypotensive treatments have been developed including pharmacological approaches and surgical outflow procedures and laser treatment. However, treatments lower IOP but are not able to halt disease progression or cure the glaucomatous lesions (Cohen and Pasquale, 2014).

1.4.1. Glaucoma and neuroinflammation

Progressive degeneration of optic nerve axons and RGCs in human glaucoma is accompanied by alterations in structural and functional characteristics in the glial cells of the retina (Tezel, 2011). Neuronal degeneration in glaucoma might be due to a combination of molecular factors such as compromised retrograde axonal transport along the optic nerve, neurotrophin deprivation, increased oxidative stress or excitotoxic stress caused by glutamate impaired response (Almasieh et al., 2012). As in neurodegenerative diseases, like Alzheimer's, Parkinson's and Huntington's diseases, glaucoma is characterized by neural cell death and inflammatory response. (Almasieh et al., 2012). The onset of the inflammatory response in glaucomatous disease is hypothesized to be mainly triggered by an altered crosstalk between RGCs and microglial cells, which in response to cell lesion highly express pro-inflammatory mediators, namely TNF, IL-1β, ROS and NO, perpetuating the neuroinflammatory milieu (Chua et al., 2012; Lee, 2013). Furthermore, in a genetic mouse model of glaucoma, DBA/2J, microglia activation was found to be an early event, even before ocular hypertension and RCG death (Bosco et al., 2011). Whether microglia activation is a cause or a consequence of glaucoma or whether it participates in the progression of the disease is yet to be clarified. Nevertheless, approaches that prevent microglia activation have been reported to be protective against RGC death (Almasieh et al., 2012; Langmann, 2007).

1.5. Adenosine

Adenosine is a ubiquitously expressed purine nucleoside that functions as a general modulator of biological functions, such as energy metabolism in the various systems throughout the body. Further research revealed other important functions of adenosine signaling in the immune system and in the CNS, being involved in cell growth, proliferation and apoptosis (Schulte and Fredholm, 2003).

Adenosine is formed intracellularly, as well as extracellularly (Fig. 5). Intracellular formation of adenosine occurs either by the breakdown of adenosine 5'-phosphate (AMP, ADP, ATP) by an intracellular 5'-nucleotidase or through the hydrolysis of S-adenosyl-homocysteine (SAH). The levels of extracellular adenosine are modulated by two different mechanisms: through nucleoside transporters or fast nucleotide hydrolysis. There are two types of nucleoside transporters, the bi-dimensional equilibrative nucleoside transporters (ENTs) that through facilitated diffusion equilibrate

theintracellular and extracellular levels of adenosine, and the concentrative nucleoside transporters (CNTs) that are capable of maintaining high concentrations of adenosine against the gradient. Adenosine can also be produced by extracellular fast nucleotide hydrolysis catalyzed by a cascade of ectoenzymes (ecto-ATPase, ecto-ATP-diphosphohydrolase and ecto-5' nucleotidase) that convert adenine nucleotides into adenosine. Furthermore, adenosine is metabolized by phosphorylation to AMP or degraded to inosine, which is then catalyzed by adenosine kinase (AK) and adenosine deaminase (ADA), respectively (Fig. 5) (Fredholm et al., 2001). Adenosine is widely distributed within the retina being found in the GCL, IPL and INL, and to a lesser extent in the photoreceptors (Blazynski et al., 1989; Braas et al., 1987).

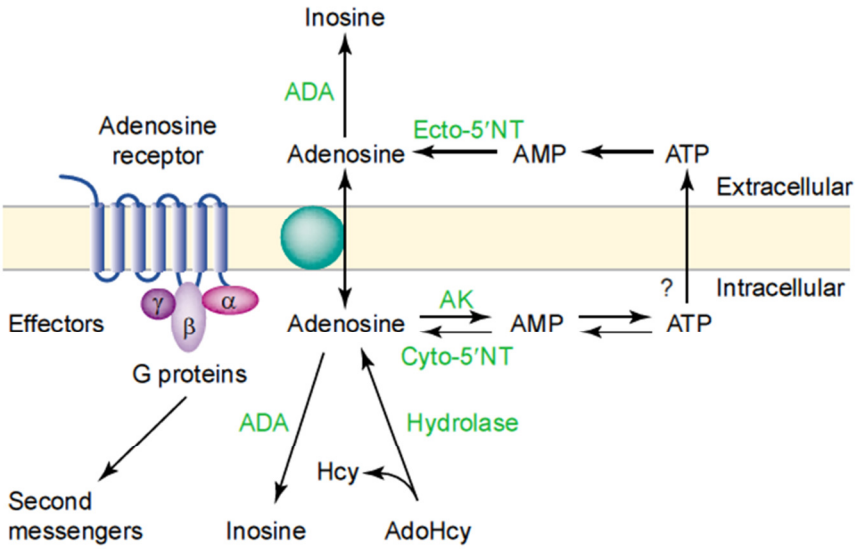

Figure 5 - Adenosine signaling pathway and metabolism. In response to cellular stress or damage, ATP is released into the extracellular space being rapidly dephosphorylated by extracellular nucleotidases to form extracellular adenosine. Ecto-5'nucleotidase (ecto-5'NT). Extracellular adenosine can interact with the four types of adenosine receptors, that regulate secondary pathways and influence cell function. Extracellular adenosine can also be deaminated to inosine by adenosine deaminase (ADA) that can exist intracellularly, or extracellular. Furthermore, adenosine can be transported into cells via facilitated nucleoside transporters. Intracellular adenosine production is generated from the dephosphorylation of AMP by a cytosolic form of nucleotidase (cyto-5'NT), or the hydrolysis of S-adenosylhomocysteine (AdoHcy). Intracellular adenosine can be secreted or phosphorylated back to ATP. The first step in this process is catalyzed by adenosine kinase (AK). Alternatively, intracellular adenosine can be deaminated to inosine by ADA. Hcy: homocysteine. Adapted from (Blackburn, 2003).

1.5.1. Adenosine receptors

Adenosine exerts its effects through the activation of four types of metabotropic membrane receptors, A_1, A_{2A}, A_{2b} and A_3. These receptors are coupled to intracellular GTP-binding proteins (G proteins) being composed of seven transmembranar domains

with the N-terminus at the extracellular and the C-terminus at the intracellular face of the membrane. All adenosine receptors (AR) are pleiotropic receptors, being able to connect to different G proteins and to different transducing systems according to their localization and degree of activation (Cunha, 2005). The AR have distinct pharmacological and functional properties. $A_{2A}R$ and $A_{2B}R$ are coupled to a stimulatory G proteins (Gs), whereas A_1R and A_3R are coupled to an inhibitory G proteins (Gi/o), stimulating or inhibiting adenylyl cyclase (AC) activity, respectively (Fredholm et al., 2001; Hasko et al., 2008; Kettenmann et al., 2011). $A_{2B}R$ and A_3R feature a parallel signaling pathway through interaction with Gq proteins, which stimulates the activity of downstream enzymes such as protein kinase C (PKC) (Fig. 6) (Hasko et al., 2008).

Adenosine receptors are expressed in microglia and are involved in the regulation their function (Cunha, 2005; Hasko et al., 2008; Kettenmann et al., 2011). Furthermore, all adenosine receptors can be found in the retina (Zhong et al., 2013) and retinal neural cell cultures where they play a key role in modulating cell response (Vindeirinho et al., 2013).

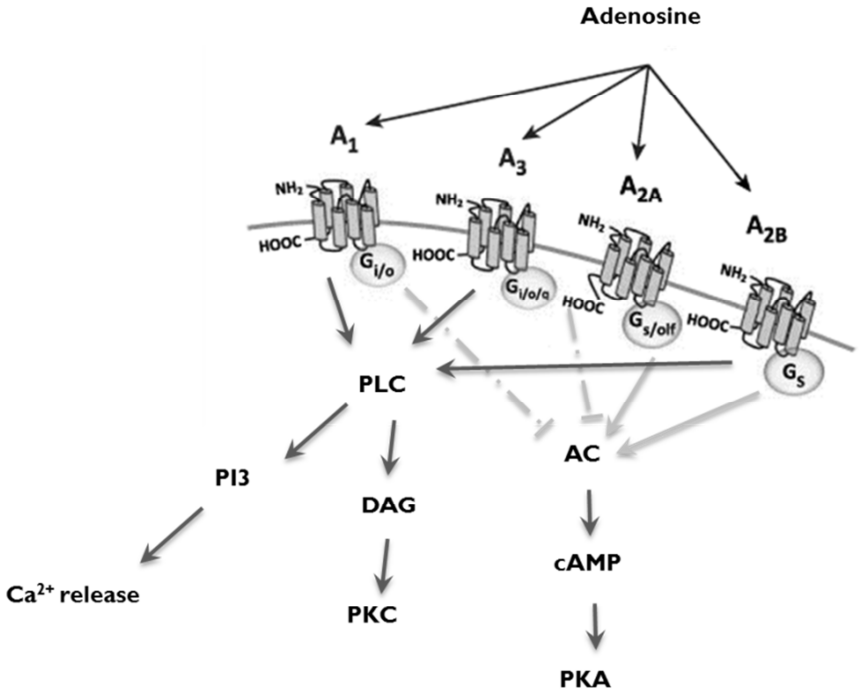

Figure 6- Schematic diagram depicting the downstream signaling pathways of adenosine receptors. Adapted from (Dias et al., 2013).

1.5.1.1. A_1 receptors

The A_1Rs are the most abundant and widespread AR in the brain, and are mostly expressed in limbic and neocortical regions (Cunha, 2005; Trincavelli et al., 2010). A_1 adenosine receptors signal through Gi/o pathways inhibiting AC. In addition, A_1R are also linked to various kinase pathways including PKC, phosphoinositide 3 (PI3) kinase and mitogen-activated protein (MAP) kinases. A_1R activation has been related to the inhibition of Ca^{2+} channels and the activation of K^+ channels (Fig. 6) (Hasko et al., 2008; Linden, 2001).

They are also present in the retina, in the NFL, GCL, IPL, the inner portion of the INL, and ONL (Zhong et al., 2013), being present in neurons synapses, in astrocytes and microglia cells (Cunha, 2005).

The neuroprotective properties of adenosine in epilepsy and against trauma and ischemia associated with brain injury have been hypothesized to be mainly mediated by the activation of A_1R (Abbracchio and Cattabeni, 1999). This function has been linked to its ability to functionally diminish the release of excitatory mediators like glutamate, acetylcholine and serotonin in presynaptic neurons and its capacity to inhibit the excitatory potential of postsynaptic neurons. Furthermore, these actions confer potent depressant, anticonvulsant and sedative properties to A_1R agonists by decreasing the metabolism rate. (Abbracchio and Cattabeni, 1999; Cunha, 2005). In RGC cell cultures, A_1R agonist increased cell survival by decreasing the excitability of post-synaptic transmission (Perigolo-Vicente et al., 2013).

The systemically administration of A_1R agonists has potentially dangerous collateral effects by inducing profound sedation, hypotension, hypothermia and cardiovascular effects. Moreover, repeatedly activation of A_1R may lead to its desensitization and loss of protective function (Abbracchio and Cattabeni, 1999).

New therapies improving the selectivity of A_1Rs in the brain open novel prospects to the treatment of neurodegenerative diseases by reducing collateral effects and the extent of desensitization (Abbracchio and Cattabeni, 1999).

1.5.1.2. A_{2A} receptors

A_{2A}R are facilitatory receptors being coupled to Gs proteins and leading to an increase in cAMP levels due to AC activity. On the other hand, increased levels of cAMP

lead to activation of protein kinase A (PKA), which follows through the phosphorylation of the transcription factor of cAMP responsive element binding protein (CREB), resulting in its activation (Fig. 6). Moreover, activated CREB can mediate gene expression showing the potential of $A_{2A}R$ to control cellular function (Hasko et al., 2008).

$A_{2A}R$ were initially identified in the striatum being localized at postsynaptic neurons and implicated in the regulation of motor functions (Cunha, 2005). Further studies show that $A_{2A}R$ is also expressed in the hippocampus and cortex being most abundant pre-synaptically. Moreover, $A_{2A}Rs$ are also located in astrocytes and microglia, as well as in blood vessels (Cunha, 2005). $A_{2A}R$ is present in the retina being expressed in the GCL, INL, ONL (Zhong et al., 2013), and in retinal microglia cells (Liou et al., 2008). Furthermore, $A_{2A}R$ has been described to be increased following exposure to noxious and upon microglia activation (Cunha, 2005; Vindeirinho et al., 2013; Wittendorp et al., 2004).

1.5.1.3. A_{2B} receptors

$A_{2B}R$ once activated acts by modulating AC activity through Gs protein signaling, which conduces to an increase in cAMP formation leading to the activation of PKA that ultimately triggers CREB phosphorylation and activation (Schulte and Fredholm, 2003). In addition, $A_{2B}R$ has also been described to activate PKC and PI3 kinase pathways through interaction with Gq protein (Fig. 6) (Hasko et al., 2008; Schulte and Fredholm, 2003). $A_{2B}Rs$ are present in different cell types like astrocytes and neurons but were not yet identified in microglia cells (Cunha, 2005). Comparing with other ARs, $A_{2B}Rs$ are less abundant and exhibiting low affinity to adenosine (Schulte and Fredholm, 2003), meaning that adenosine concentration needs to be increased to pathological levels to trigger $A_{2B}R$ activation (Hasko et al., 2008).

1.5.1.4. A_3 receptors

A_3R activation is associated with Gi/o mediated AC inhibition and Gq mediated activation of PKC. Additionally, A_3R activation modulates cell function by activation of PI3 kinase pathways (Fig. 6) (Hasko et al., 2008; Schulte and Fredholm, 2003).

The distribution of A_3Rs in the brain is very diffuse being detected in all brain areas (Abbracchio and Cattabeni, 1999). Moreover, A_3R can be found in different cell types like

neurons, microglia and astrocytes where their function is more evident (Cunha, 2005). The A_3R is also expressed in the retina being found in the RGCs and RPE (Zhong et al., 2013).

The A_3Rs are activated under specific noxious conditions since its activity is mediated by local high adenosine concentrations due to the low affinity of this receptor to adenosine. Furthermore, the A_3R is thought to easily desensitize upon stimulus (de Mendonca et al., 2000).

1.6. Neuroprotection mediated by $A_{2A}R$

Some studies indicate a controversial role for $A_{2A}R$ in inflammation. It is well documented that its activation is beneficial in peripheral inflammation conducting to an off signal (Hasko et al., 2008; Sitkovsky and Ohta, 2005), whereas in studies in CNS suggest a beneficial effect in the blockade of the $A_{2A}R$ (Rebola et al., 2011). In fact, recent research revealed a protective effect of $A_{2A}R$ blockade in neurodegenerative disorders like Huntington's disease, Alzheimer's disease, epilepsy and others (Cunha, 2005). The $A_{2A}R$, modulates the funtions of microglia, namely chemotaxis and the production and release of inflammatory mediators (Gomes et al., 2013). Under inflammatory conditions, the responses of microglia are initially protective (acute neuroinflammation) but due to a deregulated microglia response its effect become noxious (chronic neuroinflammation) and leads to neural cell death (Almasieh et al., 2012; Gomes et al., 2013; Streit, 2000). Several results show that the blockade of $A_{2A}R$ provides neuroprotection by controlling microglia reactivity (Cunha, 2005). Furthermore, unlike A_1R, the $A_{2A}R$ do not desensitize with prolonged administration of antagonists and can afford neuroprotection with considerably lower doses, producing less peripheral effects (Abbracchio and Cattabeni, 1999; Cunha, 2005). These pharmacokinetic properties make $A_{2A}R$ antagonists particular interesting targets to develop novel and effective neuroprotective drugs.

1.7. Elevated hydrostatic pressure model

Several models of RGC death and elevated pressure have been developed to try to unravel the pathophysiological mechanisms underlying glaucomatous disease. Indeed, animal models with trabecular meshwork or episcleral vein obstruction have been used to increase hydrostatic pressure in the anterior chamber (Zeiss, 2013). Furthermore, optic nerve crush and ischemia-reperfusion injury have also been used as models of RGCs

degeneration characteristic of glaucoma. Several *in vitro* models of elevated hydrostatic pressure (EHP) have been developed to assess the cells response to pressure using different time points and pressure levels, ranging from 15 mmHg to 100 mmHg above atmospheric pressure (Agar et al., 2006; Agar et al., 2000; Reigada et al., 2008; Sappington et al., 2006). Previous studies described that the exposure of eyecup's preparationss to increased hydrostatic pressure lead to an impaired glutamate signaling leading to Müller cells and retinal axonal swelling (Ishikawa et al., 2010, 2011), increased ATP release and neuronal cell death (Reigada et al., 2008). Moreover, reports in differentiated RGC cells exposed to increased pressure described that sustained moderate pressure elevation damage cell integrity by injuring mitochondria (Ju et al., 2009), increases extracellular ATP (Resta et al., 2007), and triggers oxidative stress, being an early event in hydrostatic pressure induced neuronal damage (Liu et al., 2007). Studies using co-cultures of RCG and glial cells exposed to increased hydrostatic pressure showed and increased release of TNF by glial cells and conduced to RGC death (Tezel and Wax, 2000). In our EHP model, an increase of 70 mmHg above atmospheric pressure was used, based on previous findings on microglial cell response and RGC death (Sappington et al., 2006; Sappington et al., 2009).

Aims

Glaucoma is a neurodegenerative disease characterized by RGC death and optic nerve atrophy. Elevated IOP is the main risk factor for disease development and despite IOP control current treatments are unable to prevent disease progression. Microglia-mediated neuroinflammation is an important component of glaucoma. Recent evidences suggest that the control of the inflammatory milieu has great potential to attenuate RGC loss in retinal diseases like glaucoma. The blockade of the $A_{2A}R$ has been demonstrated to afford robust neuroprotection against several brain noxious conditions by modulating microglia activation and the onset of the inflammatory response. Several approaches have been developed to unravel the pathophysiological mechanisms underlying RGC loss in glaucoma.

The aim of this work was to assess the effects of $A_{2A}R$ blockade on pressure-induced microglia activation and retinal cell death, disclosing the potential neuroprotective effects arising from SCH 58261, a selective $A_{2A}R$ antagonist (Fredholm et al., 2001).

To achieve our goals we used three experimental models: primary retinal neural cell cultures, a microglia cell line (BV-2) and retinal organotypic cultures. The cultures were submitted to 70 mmHg above atmospheric pressure to mimic the increase in IOP described in glaucoma. The expression and release of pro-inflammatory cytokines, the production of ROS, as well as cell death and microglia morphology were assessed. The role of $A_{2A}R$ blockade was evaluated pharmacologically by pre-treating the cultures with SCH 58261. Furthermore, organotypic retinal cell cultures were prepared from wild type and $A_{2A}R$-KO mice, in order to investigate the role of $A_{2A}R$ in the changes of microglia morphology upon exposure to EHP.

In summary (Fig. 7), we hypothesize that EHP elicits microglia activation increasing its proliferation, migration and the release of inflammatory mediators, like IL-1β, TNF, ROS and NO. Furthermore, we hypothesized that $A_{2A}R$ antagonist prevents EHP-induced microglia reactivity

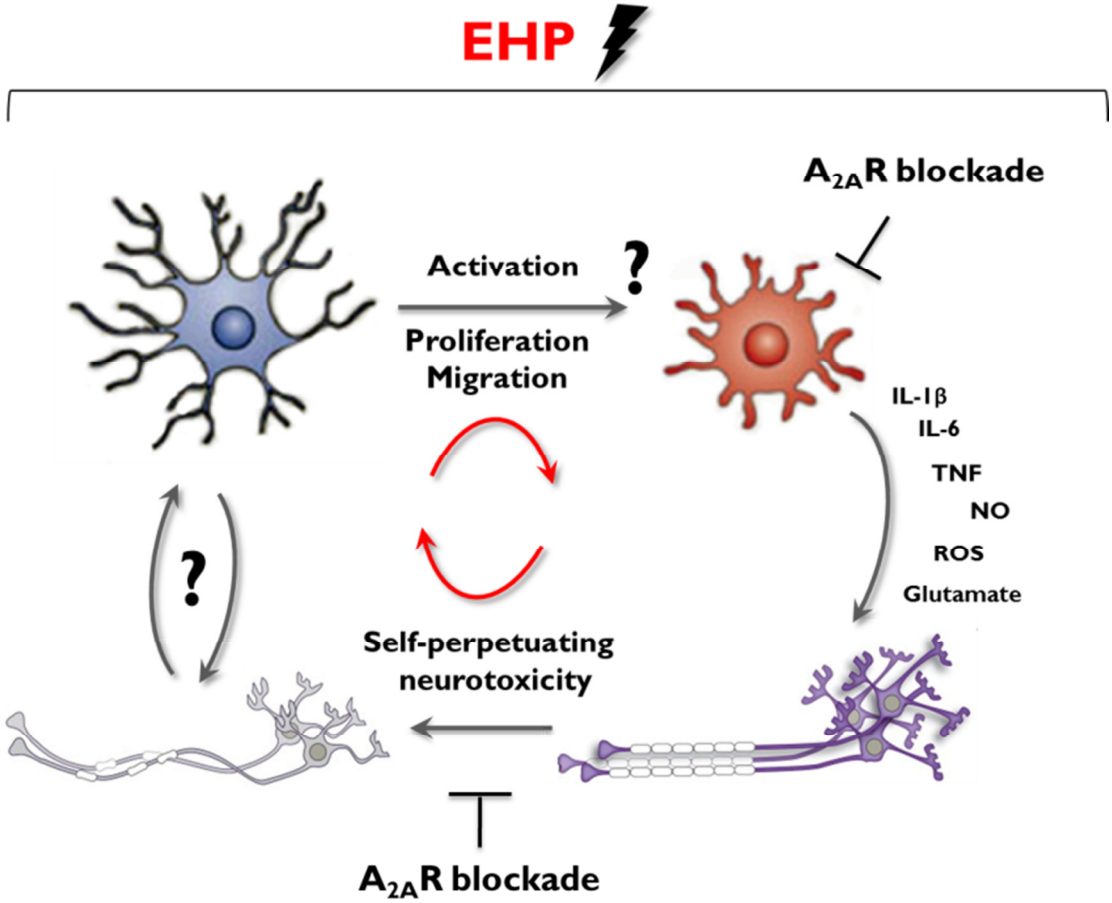

Figure 7 - Mechanisms hypothesis of the effects operated by EHP and A2AR blockade.

Chapter 2

Methods

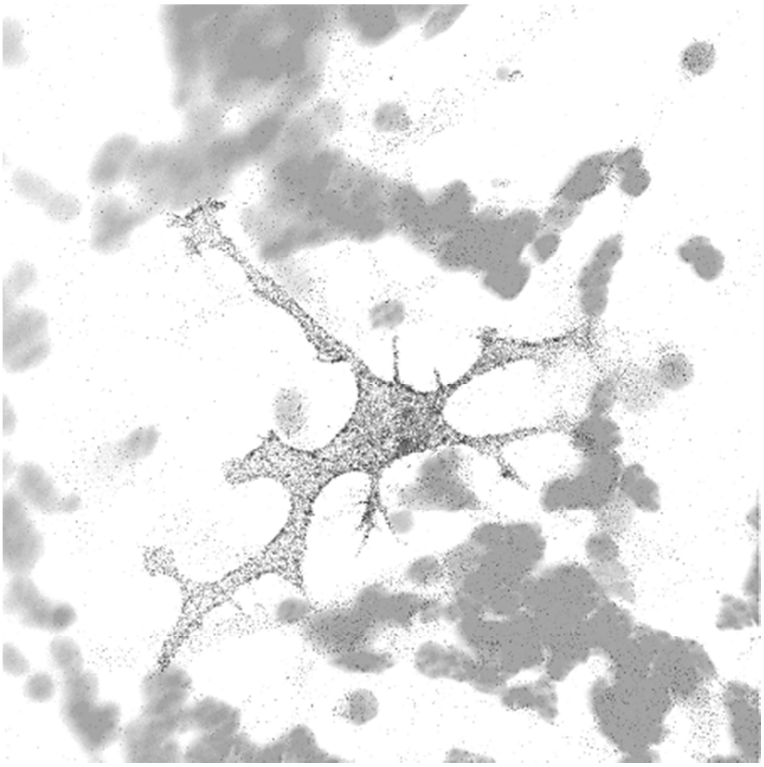

"Microglia cell – Primary retinal neural cell culture"

2. Methods

2.1. Animals

All animals used in this study, wild type mice and A_{2A}R-KO mice C57BL/6 and Wistar rats were housed under controlled environment (21.8±0.1°C of temperature and, 67.6±1.6% of relative humidity, 12 h-light/dark cycle) with free access to food and water. The animals were treated in agreement with the Association for Research in Vision and Ophthalmology (ARVO) statement for the use of animals in vision and ophthalmic research.

2.2. Mice genotyping

Tissue samples were obtained by tail biopsy in accordance with FELASA guidelines and DNA was isolated for further genotype assessment. Briefly, the tissue samples were digested using a lysis buffer solution (5 mM EDTA, 200 mM NaCl, 100 mM Tris, 0.3% sodium dodecyl sulfate (SDS), pH 8.0) and 20 mg/ml proteinase K for 4 h at 55°C. The solution was centrifuged at 13400 g for 15 min. The supernatant was collected and ice-cold 100% ethanol was added. The samples were centrifuged at 1500 g for 15 min and the supernatant was discarded. The pellet was ressuspended in 75% ethanol and centrifuged at 1500 g for 15 min. The supernatant was discarded and the samples were left to dry overnight. The pellet was then dissolved in Tris-EDTA (TE) buffer (10 mM Tris-HCl, 1 mM EDTA, pH 8.0) and heated at 70°C for 10 min. DNA concentration and purity were determined using NanoDrop ND-1000. Samples were then submitted to a standard end-point PCR using a mix of DNA polymerase (Invitrogen), dNTP's (Nzytech) and custom-designed primers (Life Technologies) (see table 1).

Tabela 1 - PCR primes sequence for genotyping

Target gene	Primer sequence
$A_{2a}R$	**F:** AGCCAGGGGTTACATCTGTG
	R: TACAGACAGCCTCGACATGTG
NEO	**F:** TCGGCCATTGAACAAGATGG
	R: GAGCAAGGTGAGATGACAGG

The PCR conditions were as follows: initial denaturation 4 min at 94°C, 30 seconds at 94°C, 30 seconds at a 55°C and 50 seconds at a 72°C for 35 cycles, and a final cycle of 7 min at 72°C. Samples were then kept at 4°C. Resulting samples were then subjected to

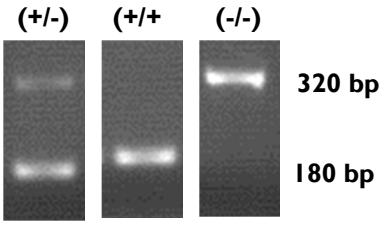

Figure 8 - Representative PCR analysis of DNA from mouse tail tissue. The specific set of primers designed for A2AR gene and for internal Neo cassette generated a 180 or 320bp, respectively.

electrophoresis in a 1.5% agarose gel with 5% ethidium bromide, at 150 v for 35 min, being then observed in a transilluminator (Versadoc, Bio-Rad) and compared with a standard ladder (NZYDNA Ladder V, Nzytech) (Fig. 8).

2.3. Primary retinal neural cell cultures

Retinal neural cell cultures were prepared from 3-5 days old rats, as described in Santiago et al. (2006). Briefly, the animals were sacrificed by decapitation being the eyes collected and kept on ice in Hanks balanced salt solution (HBSS in mM: 137 NaCl, 5.4 KCl, 0.45 KH_2PO_4, 0.34 NaHPO , 4 $NaHCO_3$, 5 glucose; pH 7.4). The retinas were dissected and the tissue was then digested with trypsin (0.1% (w/v)) for 12 min at 37°C. The cell suspension was centrifuged at 1280 g for 1 min. Supernatant was carefully discarded and the pellet was resuspended in Eagle's minimum essential medium (MEM) supplemented with 26 mM $NaHCO_3$, 25 mM HEPES, 10% heat-inactivated fetal bovine serum (FBS), penicillin (100 U/ml) and streptomycin (100 µg/ml). Cells were then plated at a density of $2x10^6$ cells/cm^2, in 12 well-plates with glass coverslips, or 6 well-plates, all pre-coated with poly-D-lysine (0.1 mg/ml). Cells were cultured at 37°C in a humidified atmosphere of 5% CO_2 for seven days. The mixed culture is composed of retinal neurons, Müller cells and microglia.

2.4. BV-2 cell line

BV-2 cells (murine microglia) were cultured in 25 cm^2 flasks in Roswell Park Memorial Institute medium (RPMI) supplemented with 10% FBS and antibiotics (penicillin 100 U/ml, streptomycin100 µg/ml). Medium was changed every 3 days.

For experiments, BV-2 cells were cultured in RPMI supplemented with 2% FBS and antibiotics (penicillin 100 U/ml, streptomycin 100 µg/ml) at a density of $6x10^4$ cells/cm^2 in 6 well plates or at a density of $4x10^5$ cells/cm^2 at 12 well plates, and cultured at 37°C in a humidified atmosphere of 5% CO_2.

2.5. Retinal explants

Retinal explants were obtained from wild type mice and A_{2A}R-KO mice C57BL/6 by enucleating the eyes and fully dissect the retina. Retinas were cultured for 4 days in culture inserts (12 mm, hydrophilic PTFE, 0.4 µm pore diameter, Millipore) in a cell incubator at 37°C in a humidified atmosphere of 5% CO_2. Retinal explants were subjected to EHP for 4 or 24 h or kept at a standard incubator (Fig. 9).

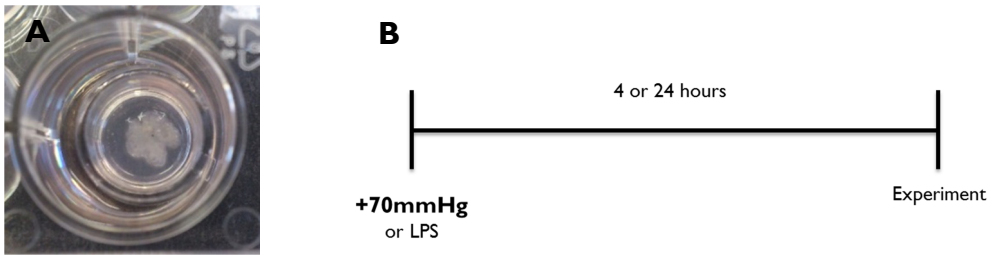

Figure 9 - (A) Image depicting organotypic retinal cell culture. (B) Schematic representation of organotypic retinal cell cultures experimental procedure.

2.6. Cell treatment

Cell cultures were pre-treated with A_{2A}R selective antagonist (50 nM, SCH 58261) 45 min before the insult. The cells were challenged with EHP (70 mmHg above atmospheric pressure) for 4 or 24 h (Fig. 10).

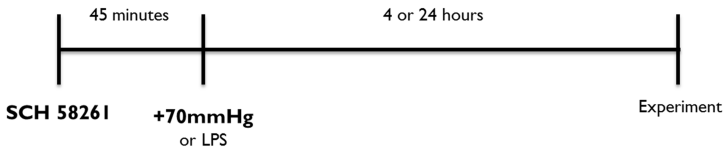

Figure 10– Schematic representation of primary mixed retinal cell cultures experimental procedure.

EHP conditions were maintained as described previously (Sappington et al., 2006). Briefly, the pressure chamber consists of a custom-made humidified pressure chamber that is equipped with a regulator and a gauge and placed in a 37°C incubator. Elevated pressure is obtained by injecting a mixture of 95% air 5% CO_2 into the chamber until +70

mmHg hydrostatic pressure is achieved (9% increase above atmospheric pressure). The EHP was continuously maintained inside the chamber (Fig. 11).

Control cultures cells were kept at atmospheric pressure in a standard incubator. In some experiments, retinal neural cell cultures and BV-2 cell cultures were treated with 1µg/ml or 100 ng/mL of lipopolysaccharide (LPS), respectively, for 24h. LPS is a component of the Gram-negative bacteria cell membrane, which is a well-characterized inflammatory stimulus able to induce microglial activation, used in this study as a positive control (Rebola et al., 2011).

Retinal neural cell cultures were incubated with 100 µM kainate (KA) and 30 µM ciclotiazide (CTZ) for 24 h as a cell death positive control.

Figure 11– Image depicting the pressure chamber. Humidified pressure chamber equipped with a regulator to ensure + 70 mmHg, and placed at 37°C.

2.7. Immunocytochemistry

2.7.1. Cell cultures

The cells was washed with warm phosphate-buffered saline (PBS; in mM: 137 NaCl, 2.7 KCl, 10 Na_2HPO_4, and 1.8 KH_2PO_4; pH 7.4) and then fixed using 4% paraformaldehyde (PFA) with 4% sucrose for 10 min. After fixation, the cells were washed with PBS and permeabilized in 1% Triton X-100 in PBS for 5 min. Next the cultures were blocked with 3% Bovine Serum Albumin (BSA) and 0.2% Tween, in PBS, for 60 min. Coverslips were then incubated with the primary antibodies (see table 2) for 90 min. Subsequently cells were rinsed with blocking solution and incubated with the secondary antibodies, (see table) for 60 min. After cells were washed with PBS and incubated with 4',6-diamidino-2-phenylindole (DAPI) (1:2000) for 10 min. The coverslips were them again washed with PBS and mounted with Glycergel mounting medium.

Tabela 2 - List of primary and secondary antibodies used in immunofluorescence labeling.

	Supplier (cat no)	Host	Dilution
Primary antibodies			
anti-Iba1	Wako (019-19741)	Rabbit	1:200
anti-iNOS	Santa Cruz (sc-650)		
anti-CD11b	Serotec (MCA275R)	Mouse	
Secondary antibodies			
Alexa fluor 488 anti-rabbit IgG	Invitrogen (A11008)	Goat	1:200
Alexa fluor 568 anti-mouse IgG	Invitrogen (A11004)		
Alexa flour 568 anti-rabbit IgG	Invitrogen (A-11011)		

2.7.2. Organotypic retinal cell cultures

Organotypic cultures were washed with PBS and fixed for 10 min with ice-cold ethanol at 4°C. Following wash in PBS, cultures were blocked with 10% goat serum, 3% BSA and 0.1% Triton X-100 in PBS, for 1 hour, and then incubated with the primary antibody against Iba-1 (Table 2) for 48 h at 4°C. After washing, cultures were incubated overnight with the secondary antibody anti-rabbit alexa fluor 568, at 4°C. Subsequently, retinas were washed and incubated with DAPI (1:1000) for 20 min. Next, retinas were washed and flat-mounted on slides and coverslipped using Glycergel mounting medium.

The preparations were observed with a confocal microscope (LSM 710, Zeiss), and 8 random fields covering the four quadrants were acquired from each condition.

2.8. Densitometric analysis of iNOS immunoreactivity

Quantitative analysis of total fluorescence in a cell was performed from images of primary retinal cell cultures immunostained for inducible nitric oxide synthase (iNOS) and CD11b. iNOS immunoreactivity was quantified using the public domain ImageJ program (http://rsb.info.nih.gov/ij/). Cell immunoreactivity was calculated using the corrected total cell fluorescence (CTCF), following the formula, as previously described in (Gavet and Pines, 2010):

$$CTCF = Integrated\ density - (area\ of\ selected\ cell \times mean\ flourescense\ background\ reading)$$

2.9. Reactive oxygen species quantification by dihydroethidium staining

The production of ROS was assessed by dihydroethidium (DHE) staining. DHE is a probe that is oxidized to ethidium in the presence of the superoxide anion (O^{2-}) and intercalates with DNA emitting red fluorescence that can be observed by microscopic analysis. Briefly, cell medium was collected and the cells were incubated with 5 μM DHE in fresh culture medium for 1h in the cell incubator. Then, the medium was replaced by the previous collected medium and the cells were cultured for 4h. The cell cultures were rinsed with warm PBS, fixed, and immunostained for CD11b, as previously described. Cells were observed with a confocal microscope (LSM 710, Zeiss), and from each condition 5 random fields were acquired. The number of CD11b-immunoreactive cells stained with DHE per field was counted.

2.10. Nitrite quantification assay

The production of NO in primary retinal cell cultures was assessed by the Griess reaction method. The culture medium was collected and centrifuged to remove cell debris and then incubated (1:1) with Griess reagent mix (1% sulfanilamide, in 5% phosphoric acid with 0.1% N-1-naphtylenediamine) for 30 min, protected from light. The optical density was measured at 550 nm using a microplate reader (Synergy HT; Biotek, Winooski, USA). The nitrite concentration was determined by comparison to a sodium nitrite standard curve.

2.11. Assessment of cell morphology

Morphological alterations were assessed using an automated feature of ImageJ as previously described (Kurpius et al., 2006). First, threshold was arbitrarily but uniformly applied to confocal images labeled with CD11b. Next, the particle measurement feature of ImageJ (http://rsb.info.nih.gov/ij/) was used to automatically measure the 2D area, perimeter, Feret's diameter and circularity index. A circularity value of 1.0 indicates perfect circular cell and values near to zero indicate elongated cells. Feret's diameter is the greatest distance between two points along the perimeter.

2.12. Cell proliferation assay

Cell proliferation was assessed using the Click-iT® EdU cell proliferation assay according to the instructions provided by the manufacturer (Life Technologies). The principle of the kit is the incorporation of a nucleoside analog of thymidine, EdU (5-ethynyl-2´-deoxyuridine), into DNA in the S phase of the cell cycle. EdU is coupled to a fluorophore (Alexa Fluor 488) for microscope vizualization. Briefly, half of the culture medium was replaced by fresh medium containing the EdU solution (final concentration of 10 μM) and incubated for 24h until the end of the experiment. Cells were rinsed, fixed, permeabilized and blocked as previously described. Next, cells were incubated for 30 min with the Click-iT® reaction cocktail, followed by immunostaining for CD11b as previously described. Nuclei were stained with Hoechst 33342 (1:2000). Cells were observed with a confocal microscope (LSM 710, Zeiss), and from each condition, 5 random fields were acquired. The number of EdU-positive cells was counted. Results represent the average of EdU-positive cells per field and the percentage of CD11b-positive cells stained with EdU.

2.13. Terminal deoxynucleotidyl transferase (TdT)-mediated dUTP nick end labeling (TUNEL) assay

To detect apoptotic cells DeadEnd™ Fluorometric TUNEL System was used following manufacturer's instructions (Promega). TUNEL assay assesses cell apoptosis by labeling DNA fragments by catalytically incorporating fluorescein-12-dUTP at 3´-OH DNA ends using the recombinant Terminal Deoxynucleotidyl Transferase (rTdT). Cultures were immunostained for CD11b and then incubated with TUNEL reaction cocktail for 60 min at 37°C. The nuclei were then stained using DAPI (1:2000). Cells were observed with a confocal microscope (LSM 710, Zeiss), and from each condition, 5 random fields were acquired. The total number of TUNEL-positive cells and the number of CD11b-immunireactive cells stained with TUNEL were counted. Results represent the average of TUNEL-positive cells per field and the percentage of CD11b-positive cells marked with TUNEL in the cytoplasm.

2.14. Phagocytosis assay

Phagocytosis was assayed with fluorescent latex beads (1 μm diameter), as previously described (Pan et al., 2011) with minor modifications as follows, BV-2 cells were

incubated with 0.025% beads for 60 min at 37°C. Then, the cells were fixed, permeabilized and blocked. Primary cultures were processed for immunostaining anti-CD11b as described previously, and BV-2 cells were stained with Phalloidin conjugated to Tetramethylrhodamine B isothiocyanate (TRITC) (1:500; Sigma-Aldrich). Phalloidin selectively binds to F-actin, allowing visualization of BV-2 cells. Nuclei were stained with DAPI (1:2000). Cells were observed with a confocal microscope (LSM 710, Zeiss), and from each condition, 5 random fields were acquired. The number of beads phagocytized by each cell was counted as well as the number of cells with incorporated beads. Phagocytic efficiency (%) was then calculated as described in (Pan et al., 2011):

$$Phagocytic\ efficiency\ (\%) = \frac{(1 \times x1 + 2 \times x2 + 3 \times x3 \ldots + n \times xn)}{total\ number\ of\ cells} \times 100\%$$

xn represents the number of cells containing n microspheres (n = 1,2,3, ... up to a maximum of 6 points for more than 5 microspheres ingested per cell).

2.15. Scratch wound assay

Confluent BV-2 cells, plated in 6-well plates, were wounded with a sterile p200 pipet tip and after washing to remove non-adherent cells, then were cultured for 4h. As previously described in (Yuskaitis and Jope, 2009) with minor modifications. Images were acquired before, immediately and 4h after the wound (Fig. 12) with an inverted fluorescence microscope (LEICA DMIRE2). The number of cells in the wound was

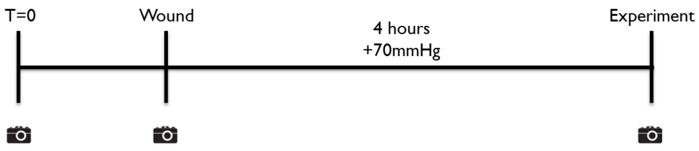

Figure 12 – Schematic representation of Scratch wound assay experimental procedure. Images were acquired in tree points as depicted. Cells were plated, wounded with a sterile p200 pipet tip and cultured for 4h under EHP.

counted.

2.16. Boyden chamber migration assay

BV-2 cells were kept in serum free medium 24h before the beginning of the experiment and plated with 2% FBS serum in transwell cell culture inserts (8.0 µm pore

diameter, Merck Millipore) at a density of $3x10^4$ cells/cm^2 and were cultured for 4 h, as described in (Yuskaitis and Jope, 2009) with some modifications (Fig. 13).

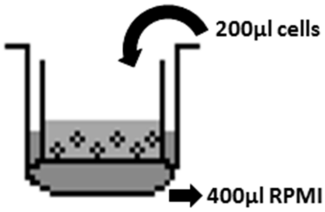

Figure 13 - Schematic representation of Boyden chamber migration assay experimental procedure. Cells were plated in the upper side of the transwell cell culture inserts and submitted to EHP for 4h.

Culture inserts were then washed with warm PBS and the cells in upper side were removed with a cotton swab, following fixation in 4% PFA with 4% sucrose for 10 min. Nuclei were stained with DAPI (1:2000) to allow cell counting, as described (Siddiqui et al., 2012). The membrane was removed and mounted with Glycergel in glass slides. The preparations were observed in an inverted fluorescence microscope (LEICA DMIRE2) and 5 random images per insert were acquired. The number of cells in the bottom side of the insert (the cells that migrated) was counted.

2.17. Determination of adenosine concentration by high performance liquid chromatography

Extracellular adenosine was quantified using high performance liquid chromatography (HPLC), with detection at 254 nm, as previously described in (Vindeirinho et al., 2013). Briefly, cell culture medium was collected and immediately stored at -80°C until further processing. The samples were then analyzed in Beckman-System Gold, HPLC apparatus, with a computer controlled 126 Binary Pump Model using a 166 Variable UV detector and a Lichrospher 100 RP-18 (5 mm) from Merck column. An isocratic elution with 10 mM phosphate buffer (NaH_2PO_4; pH 6.0) and 14% methanol was performed with a flow rate of 1.5 ml/min. Adenosine was quantified by retention time, absorption spectra and comparison with the standard curve. Results were presented in pmol/µg of protein which was quantified by bicinchoninic acid (BCA) protein assay (Pierce Biotechnology).

2.18. Determination of ATP concentration by luciferin-luciferase bioluminescence assay

The extracellular levels of ATP were quantified using the luciferin-luciferase bioluminescence assay. This method is based on the enzymatic reaction which converts luciferin to its oxidated form luciferase in the presence of ATP, being this response dependent to the ATP availability and allowing the assessment of ATP concentrations ranging between $2x10^{-12}$ M and $8x10^{-5}$ M. This reaction leads to light emission at 565 nm proportional to ATP levels, which were measured using a VICTOR multilabel plate reader (Perkin Elmer). Briefly, cell medium was collected and immediately stored at -80°C, until used. Samples were quickly defrosted and incubated with ATP assay mix (Sigma-Aldrich), designed for bioluminescence, in an opaque white 96-well plate. The plate was then read at luminometer for 5 seconds. ATP concentrations were determined by comparison with a standard curve obtained from an ATP sock provided. Results are presented pmol/µg of protein which was quantified by BCA protein assay (Pierce Biotechnology).

2.19. RNA extraction

The cells were washed with ice-cold autoclaved PBS and then lysed with TRIZOL reagent (Life Technologies). Cell monolayer was then disrupted using a p1000 pipet tip, collected and kept overnight at -80°C. Samples were then defrosted and chloroform was added being the tubes vigorously shaken to promote homogenization of the mixture and incubated for 5 min on ice. Then samples were centrifuged at 12000 g for 15 min at 4°C to assure phase distribution. Upper aqueous phase was collected to a new tube and RNA was precipitated with isopropanol. Glycogen (20 µg) (Invitrogen, Life Technologies) was added as a carrier to facilitate precipitation. Samples were kept at -20°C overnight, and then centrifuged at 12000 g for 30 min at 4°C. The pellets were washed twice with ethanol, and RNA was resuspended in RNase-free water. RNA concentration and purity were determined using NanoDrop®. Resulting RNA samples were treated with Deoxyribonuclease I (DNase I) (amplification grade, Invitrogen, Life Technologies) to eliminate possible contamination with genomic DNA.

2.20. Reverse transcription

RNA samples were reversed transcribed to cDNA using NZY M-MuLV First-Strand cDNA Synthesis Kit, according to supplier's instructions (NZYTech). Briefly, RNA was incubated for 10 min at 25°C with NZYRT 2x Master mix and NZYRT Enzyme Mix, followed by a 30 min step at 50°C and a final step at 85°C to stop the reaction. The cDNA obtained was then treated with RNAse H for 20 min at 37°C to eliminate the remaining RNA-DNA hybrids. To confirm cDNA synthesis and purity a standard end-point PCR for β-actin, using intron-spanning primers (table 3), using 2x MyTaq Red Mix (Bioline), was performed. Briefly, 1 µl of cDNA was incubated with 2x MyTaq Red Mix under the following conditions: 1 min initial denaturation at 95°C, followed by 35 cycles of denaturation at 95°C for 15 seconds, annealing at 55°C for 15 seconds, elongation at 72°C for 10 seconds. Resulting samples were then subjected to electrophoresis in a 1.5% agarose gel with 5% ethidium bromide, at 150v for 35 min, being then observed in a transilluminator (Versadoc, Bio-Rad). The cDNA samples were diluted 1:2 and kept at -20°C until further qPCR analysis.

Tabela 3 - Primers used for qPCR.

Target gene	Primer sequence	Melting temperature
YWHAZ	F:CAAGCATACCAAGAAGCATTTGA R:GGGCCAGACCCAGTCTGA	60°C
HPRT	F:ATGGGAGGCCATCACATTGT R:ATGTAATCCAGCAGGTCAGCAA	58°C
TBP	F:ACCAGAACAACAGCCTTCCACCTT R:TGGAGTAAGCCCTGTGCCGTAAG	58°C
$A_{2a}R$	F:GGCTATCTCTGACCAACA R:TGGCTTGACATCTCTAATCT	60°C
iNOS	F:AGAGACAGAAGTGCGATC R:AGATTCAGTAGTCCACAATAGTA	60°C
IL-1β	F:CTGTCTGACCCATGTGAG R:TTGTCGTTGCTTGTCTCT	60°C
TNF	F:CCCAATCTGTGTCCTTCT R:TTCTGAGCATCGTAGTTGT	60°C
β-Actin	F: GCTCCTCCTGAGCGCAAG R:CATCTGCTGGAAGGTGGACA	60°C

2.21. Real-time quantitative PCR

Cell cultures mRNA expression was quantified by qPCR in a 7500 Real-Time PCR System (Applied Biosystems) using SYBR Green to detect the amplification products. Samples were plated with SYBR Green (BioRad) and pre-optimized, custom-designed primers (Sigma-Aldrich), see table 3.

The plate was then submitted to the following protocol (Fig. 14):

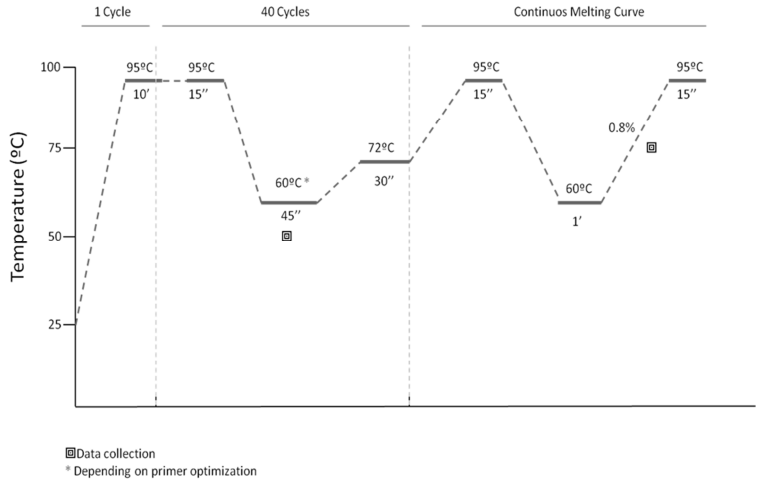

Figure 14 – Schematic representation of the qPCR cycles temperature profile.

Three housekeeping candidate genes were tested, namely YWHAZ, HPRT and TBP. All samples were analyzed using NormFinder (Andersen et al., 2004), and the most stable gene among all samples and conditions was used as housekeeping gene. In our conditions, YWHAZ was the most stable gene. Relative quantification of mRNA expression was calculated by the comparative cycle threshold (Ct) method after the target genes levels were normalized to the expression of YWHAZ for each sample. The fold difference in gene expression between treated groups was calculated as follows:

$$Fold\ difference = 2^{-\Delta\Delta Ct}$$

Where, ΔΔCt:

$$\Delta\Delta Ct = (Ct\ target - Ct\ YWHAZ)treated\ sample - (Ct\ target - Ct\ YWHAZ)control\ sample$$

2.22. Quantification of pro-inflammatory cytokines

T The quantification of IL-1β and TNF was performed using enzyme-linked immunosorbent assay (ELISA), in accordance with the manufacturer's instructions. Briefly, culture medium was collected and kept at -80°C until further analysis. To perform the

quantification the samples were defrosted and kept on ice, all the reagents needed for this assay were kept at room temperature.

IL-1β levels were quantified in retinal neural cell cultures growth medium after exposure to 4 and 24 h EHP, using Peprotech ELISA kit. Briefly, a 96-well plate was coated with the capture antibody overnight, next the plate was washed 4 times and a standard curve was prepared and loaded into the plate as well as the samples. The plate was left overnight at 4°C. The samples were removed and the plate was washed 4 times following incubation with the detection antibody for 2h at room temperature. The plate was again washed and incubated with avidin peroxidase for 30 min. After a final wash, the reaction subtract was added to each well. Readings of the OD were collected for 2h in 5 min intervals at 405 nm with wavelength correction set at 650 nm, using a microplate reader (Synergy HT; Biotek, Winooski, USA).

TNF and IL-1β level´s in BV-2 cell culture medium exposed to 24h LPS, 4h and 24h EHP, using R&D Systems ELISA kit. The procedure was the following: a standard curve was prepared to allow quantification of the samples by comparison, samples and standards were then placed in a 96-well plate, pre coated provided with the kit, and incubated for 2 h at room temperature. The plate was washed 5 times and incubated with the conjugate, provided with the kit. After 2h the plate was washed and the substrate solution was added to each well and incubated for 30 min, protected from light. Following this, stop solution was added and the optical density was measured at 540 nm or 570 nm, to corrected readings, using a microplate reader (Synergy HT; Biotek, Winooski, USA). Results are expressed as percentage of control or in pictograms per milliliter (pg/ml).

2.23. Preparation of frozen retinal sections

Animals were deeply anesthetized with an intraperitoneal injection of a solution of ketamine (90 mg/kg; Imalgene 1000) and xylazine (10 mg/kg; Ronpum 2%) and then transcardially perfused with phosphate-buffered saline (PBS, in mM: 137 NaCl, 2.7 KCl, 10 Na_2HPO_4, 1.8 KH_2PO_4; pH 7.4) followed by 4% PFA. The eyes were enucleated and post-fixed in 4% PFA for 1h. Then, the cornea and the lens were carefully dissected out and the eyecup was fixed for an additional 1 hour in 4% PFA. After washing in PBS, the tissue was cryopreserved in 15% sucrose in PBS for 1h followed by 30% sucrose in PBS for 1h. The eyecups were embedded in tissue-freezing medium (Optimal Cutting Temperature, OCT; Shandon Cryomatrix, Thermo Scientific) with 30% of sucrose in PBS (1:1), and

stored at -80°C. The tissue was sectioned on a cryostat (Leica CM3050 S) into 16 µm thickness sections and mounted on Superfrost Plus glass slides (Menzel-Glaser, Thermo Scientific). Glass slides were dried overnight and then stored at -20°C.

2.24. Assessment of retinal structure

After defrosting the slides at room temperature overnight, the sections were rehydrated in PBS twice (5 min). Then the sections were incubated with hematoxylin solution for 3 min, followed by a superficial wash (3 seconds) with HCl 0.1% solution. The sections were washed in running tap water for 5 min, and then incubated with 0.5% eosin in 100% ethanol for 3 min. The sections were then washed in running tap water for 30 seconds and then dehydrated in ascending alcohol solutions (95% and 100%, 1 min each). Then, sections were cleared through 2 changes of xylene (5 min). Finally, tissue sections were mounted with DPX mounting medium (FLUKA).

2.25. Statistical analysis

Results are presented as mean ± SEM. Statistical significance was determined using a non-parametric Kruskall-Wallis test, followed by Dunn's multiple comparison test or a non-parametric Mann-Whitney test. Groups were considered significantly different for $p<0.05$.

Chapter 3

Results

"Microglia cell – BV-2 cell line"

3. Results

Elevated IOP is the main risk factor for glaucoma. We aimed to investigate, using an *in vitro* system, the alterations induced by EHP in microglia. Therefore, elevated IOP was mimicked *in vitro* by exposing the cells to EHP (70 mmHg above atmospheric pressure) for 4 hours and 24 hours. In addition, in several experiments, we also investigated the role of $A_{2A}R$ blockade in the control of microglia responses.

Cells were also incubated with LPS, a component of Gram-negative bacteria wall, that acts through toll-like receptor 4 (TLR4) in immune cells. Accordingly, the LPS condition was mostly used as a "control" of the inflammatory cells response, because it is widely known that microglia become reactive upon TLR4 activation (Hines et al., 2013). Therefore the results obtained in this condition were not considered for statistical purposes.

3.1. Effect of elevated hydrostatic pressure in the expression of $A_{2A}R$ in primary retinal neural cell cultures

Primary retinal neural cell cultures were challenged with LPS (1 µg/ml) or EHP for 4 hours or 24 hours and $A_{2A}R$ mRNA expression was assessed by qPCR (Fig. 15). LPS increased the transcript levels of $A_{2A}R$ by 9.1±5.1 fold. Exposure to EHP for 4h and 24h changed the transcript levels of $A_{2A}R$ to 1.6 ± 0.8 and 3.2 ± 2.1 fold, respectively.

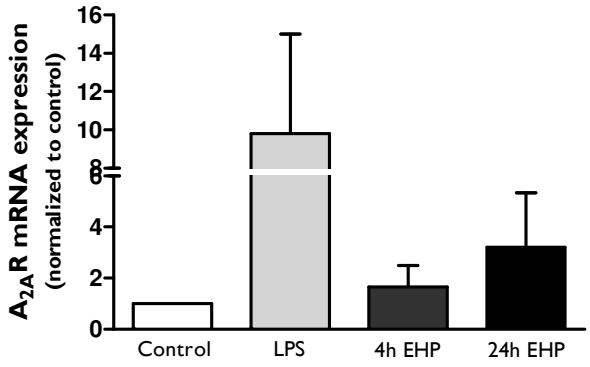

Figure 15 - Effect of elevated hydrostatic pressure in the expression of A2AR in primary retinal neural cell cultures. Primary mixed retinal cultures where challenged with 1 µg/ml LPS or EHP for 4 or 24 hours and $A_{2A}R$ mRNA expression was assessed by qPCR. Results are expressed in fold change of control, from 3 to 4 independent experiments, performed in duplicate.

3.2. Elevated hydrostatic pressure increases oxidative/nitrosative stress in primary retinal cultures

Oxidative stress caused by increased production of ROS and NO has been described as a major hallmark in glaucomatous neurodegeneration (Tezel et al., 2007). The effect of EHP on the expression of iNOS and NO production was evaluated in primary retinal neural cell cultures. In addition, the effect of $A_{2A}R$ blockade was also investigated by incubating the cells with 50 nM SCH 58261, a selective $A_{2A}R$ antagonist, prior the exposure to EHP. In control conditions, iNOS immunoreactivity was barely detected but when the cells were incubated with LPS the immunoreactitivy of iNOS, as expected, was increased, mainly in CD11b-immunorreactive cells, a marker of microglia (Fig. 16A). In order to compare the magnitude of the cells' response between LPS and EHP, the microscope settings were kept identical. When the cells were exposed to EHP for 24h the immunoreactivity of iNOS in microglia significantly increased by 192.8±28.3% of the control ($p<0.05$), as compared with the control (Fig. 16A and B). When the cells were treated with $A_{2A}R$ antagonist, the immunoreactivity of iNOS was similar to the control. We also evaluated the expression of iNOS by qPCR (Fig. 16C). Preliminary results show that the transcript levels of iNOS increased after 24 hours of EHP (2.3±1.1) and the blockade of $A_{2A}R$ may inhibit this alteration (0.4±0.2). The production of NO was assessed by quantifying nitrites in cell culture medium by the Griess reaction method. In control conditions, nitrite concentration was 4.1±0.2 μM (Fig. 16D) and incubation with LPS increased nitrite concentration to 320.2±23.2% of the control. Exposure of the cells to EHP for 24 hours significantly increased nitrite concentration to 129.5±13.7% of control ($p<0.01$). The blockade of $A_{2A}R$ significantly prevented the effect of EHP on nitrite concentration ($p<0.05$).

To investigate whether EHP changes oxidative stress, primary retinal neural cell cultures were exposed for 4h to EHP and the production of ROS production was evaluated with DHE. Incubation with LPS for 4h increased the number of cells stained with DHE (Fig. 17A). When the cells were exposed to EHP for 4h, the number of cells stained with DHE significantly increased ($p<0.01$) to 29.5±7.9 cells per field (Fig. 17B), which corresponds to a 2.5-fold increase, compared with the control.

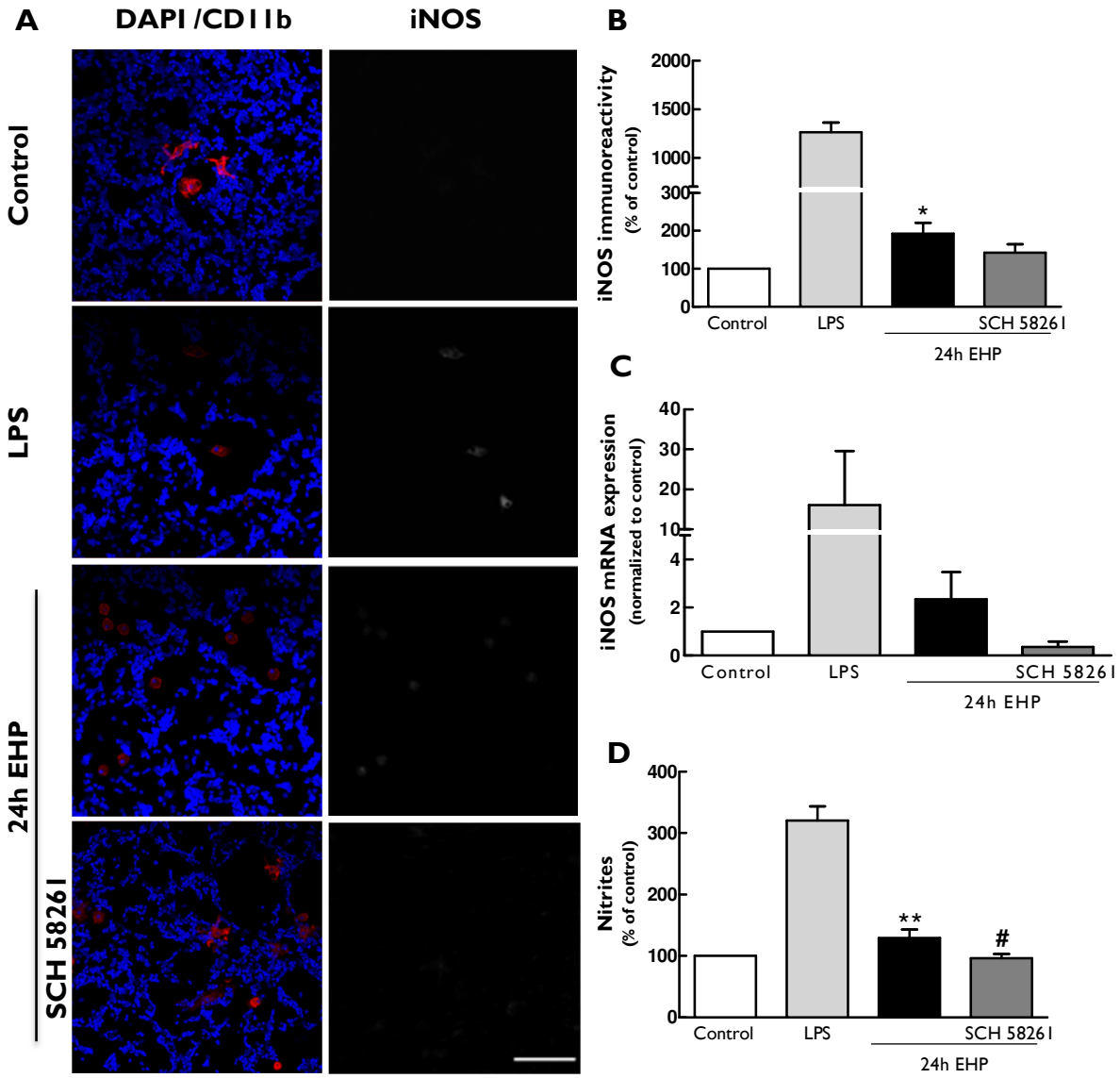

Figure 16 - Elevated hydrostatic pressure increases oxidative stress in primary retinal cultures. Primary mixed retinal cultures were pre-treated with 50 nM SCH 58261, followed by 1 µg/ml LPS or EHP for 24 hours. (A) Representative images of microglia stained with CD11b (red) and iNOS (green). Nuclei were stained with DAPI (blue). (B) Densitometric analysis for iNOS immunoreactivity was determined using ImageJ, and results are expressed in percentage of control, from 4 to 5 independent experiments, performed in duplicate. (C) iNOS mRNA expression was assessed by qPCR. Results are expressed in fold change of control from 3 to 4 independent experiments, performed in duplicate. (D) Nitrite concentration was determined in culture medium supernatants, and was expressed in percentage of control, from 5 to 6 independent experiments, performed in duplicate. *p<0.05, **p<0.01, ***p<0.001, Kruskall-Wallis test, followed by Dunn's multiple comparison test. Bar: 100 µm.

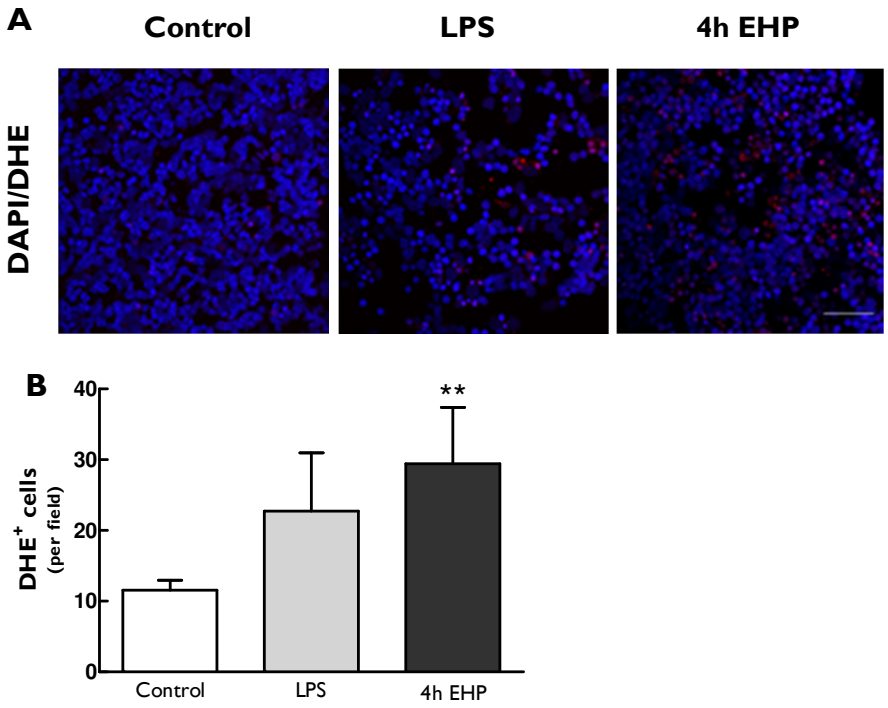

Figure 17 - Elevated hydrostatic pressure increases ROS production in primary mixed retinal cultures. The production of ROS in retinal primary mixed cultures was assessed with DHE probe after 4 hours with 1 µg/ml LPS or EHP. (A) Representative images of DHE staining (red). Nuclei were stained with DAPI (blue). (B) The number of DHE-labeled cells was counted, and the results are expressed as percentage of control, from 3 to 5 independent experiments. *p<0.05, Kruskall-Wallis test, followed by Dunn's multiple comparison test. Bar: 20 µm.

3.3. Effect of elevated hydrostatic pressure in the expression and release of TNF and IL-1β in primary mixed retinal neural cell cultures

We evaluated whether the exposure of primary retinal neural cell cultures to EHP changed the expression and release of pro-inflammatory cytokines TNF and IL-1β, by qPCR and ELISA, respectively. In cultures exposed to EHP for 4h, the expression of IL-1β transcript levels by qPCR was not different from the control due to the variability of the results and inferences can not be made. These effects were not noticeable in cultures exposed to EHP for 24h where the transcript levels of IL-1β were kept similar to control (0.9 ± 0.8) fold (Fig. 18A). Nevertheless, the levels of extracellular IL-1β assessed by ELISA were altered by the exposure to EHP for 4h being significantly increased to 233.0±70.9% of control ($p<0.05$). Furthermore when the cells were exposed for 24h to EHP, IL-1β levels increased to 167.9±45.6% of control. In control conditions the levels of IL-1β were 275.2±58.6 pg/ml (Fig. 18B). The effect of LPS for 24h was similar to 4h EHP (228.0±55.3% of the control).

TNF mRNA expression levels were also quantified using qPCR (Fig. 18C). LPS increased TNF mRNA expression by 10.9± 6.1 fold. Preliminary results suggest that EHP may change the expression of TNF after 4h or 24h exposure to EHP.

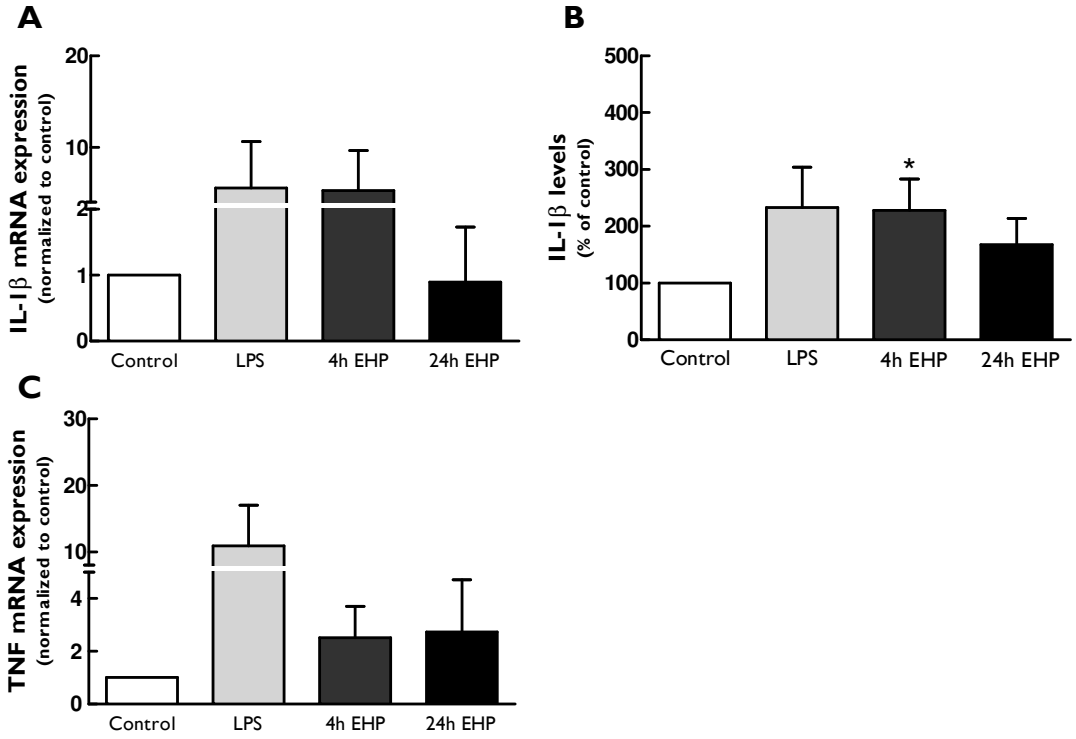

Figure 18 - Effect of elevated hydrostatic pressure in the expression and release of TNF and IL-1β in primary mixed retinal neural cell cultures. Primary mixed retinal cultures were challenged with EHP for 4 hours or 24 hours or 1 μg/ml LPS for 24 hours. IL-1β (**A**) and TNF (**B**) mRNA expression was assessed by qPCR and results are expressed as fold change of control, from 3 to 4 independent experiments, performed in duplicate. (**C**) Extracellular levels of IL-1β were quantified by ELISA in cell culture medium supernatants, and the results are expressed as percentage of control, from 3 to 4 independent experiments. *p<0.05, Kruskall-Wallis test, followed by Dunn's multiple comparison test.

3.4. Effect of $A_{2A}R$ blockade cell death induced by elevated hydrostatic pressure in retinal neural cell cultures

Primary retinal neural cell cultures were exposed to EHP for 4h and 24h and cell death was evaluated by TUNEL assay. Cells were pre-treated with $A_{2A}R$ antagonist (50 nM SCH 58261). Glutamatergic excitotoxicity is known to induce cell death to retinal neurons (Ishikawa, 2013). Therefore, cells were incubated with 100 μM kainate (KA) and 30 μM cyclothiazide (CTZ) for 24h to induce an excitotoxic insult (positive control of cell death).

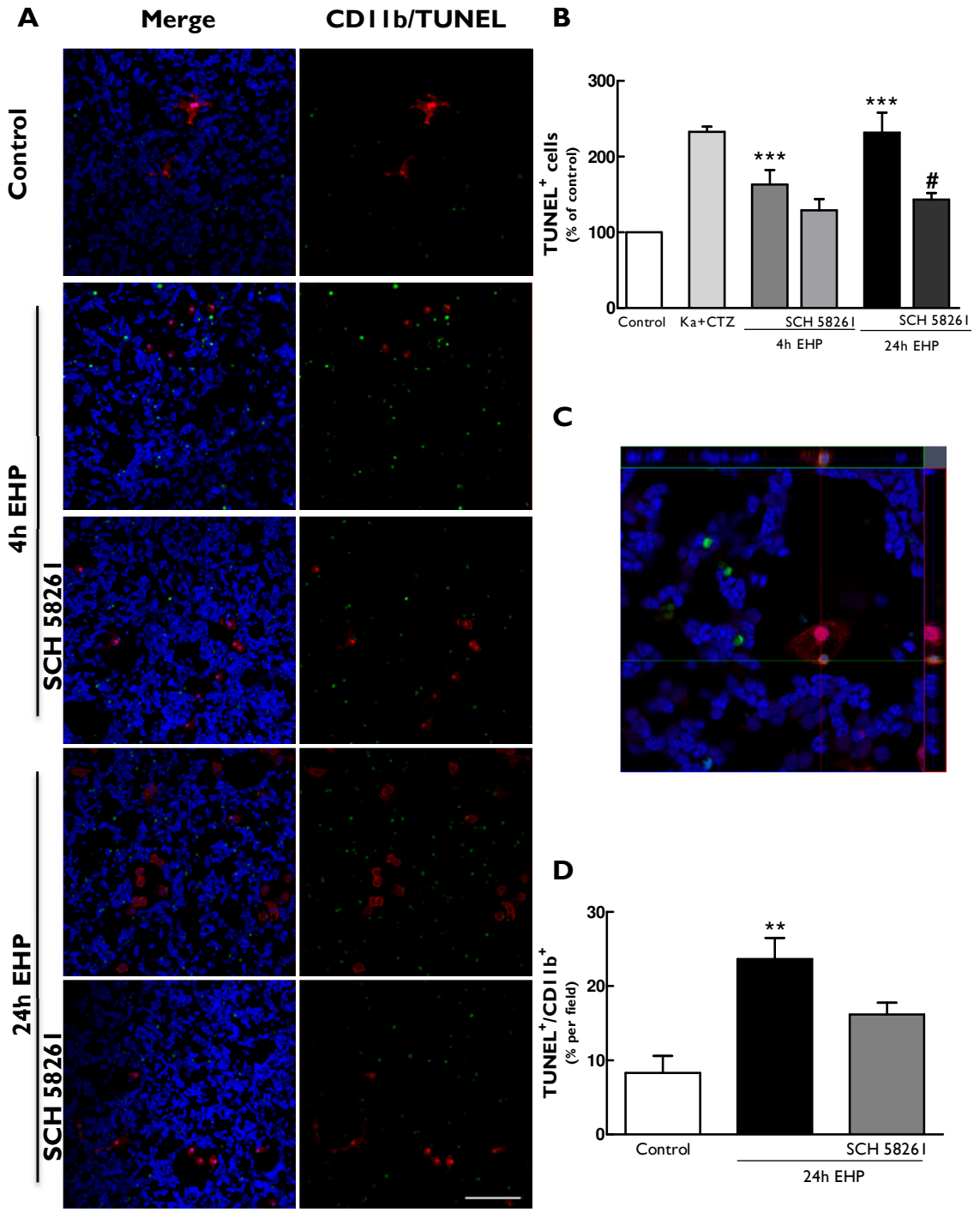

Figure 19- The effect of A2AR blockade in elevated hydrostatic pressure induced cell death and dead cells engulfment by microglia in primary mixed retinal neural cell cultures. Primary mixed retinal cultures were pre-treated with 50 nM SCH 58261 and challenged with EHP for 4 or 24 hours. As a positive control cell cultures were incubated with 100μM kainate (KA) and 30μM cyclotiazide (CTZ) for 24 hours. Cell death was assessed with TUNEL (green) assay. Microglial cells were identified by immunocytochemistry with anti-CD11b (red). Nuclei were counterstained with DAPI (blue). Representative images are depicted in **A**. (**B**) The number of TUNEL$^+$ was counted and results are expressed as percentage of control, from 6 to 9 independent experiments, performed in duplicate. (**C**) Orthogonal image representing microglial engulfment of a TUNEL$^+$ cell. (**D**) The number of microglial cells (CD11b-immuoreactive cells) with engulfed TUNEL$^+$ cells (CD11b$^+$/TUNEL$^+$) was counted per field, and the results are expressed as the percentage of total microglial cells per field, from 5 to 6 independent experiments, performed in duplicate. *p<0.05, **p<0.01, ***p<0.001, Kruskall-Wallis test, followed by Dunn's multiple comparison test. Bar: 100 μm.

Exposure of primary retinal neural cell cultures to EHP for 4h or 24h significantly increased ($p<0.001$) the number of TUNEL$^+$ cells to 163.4±18.9% and 231.5±26.7% of control, respectively. Blockade of $A_{2A}R$ prevented the increase in cell death induced by EHP at 4h and 24h to 129.3±14.8% and 143.3±8.9% of control, respectively (Fig. 19A and B). Microglia (CD11b$^+$) with TUNEL staining in the nucleus were rarely observed. However, we observed that microglial cells had TUNEL staining (Fig. 19C) suggesting that microglia are phagocytizing cell debris and apoptotic cells as previously described (Ferrer-Martin et al., 2014; Jones et al., 1997; Petersen and Dailey, 2004). The number of microglia with engulfed TUNEL$^+$ cells was significantly increased upon exposure to EHP for 24h (23.7±2.8 cells per field). The treatment with the $A_{2A}R$ antagonist prior exposure to EHP for 24h did not significantly change the number of microglia with engulfed dead cells (16.2±1.6 cells per field), as compared with control (8.3 ± 2.3 cells per field) (Fig. 19D).

3.5. Elevated hydrostatic pressure changes microglia morphology

It is widely accepted that the morphology of microglia changes accordingly to their reactive phenotype. Microglial cells were identified with an antibody anti-CD11b and several morphological parameters were evaluated. In control conditions microglia cells were ramified (Fig. 20A and table 4). Exposure of primary retinal neural cell cultures to EHP for 24h significantly decreased the area (Fig. 20B), perimeter (Fig. 20C) and Feret's diameter (Fig. 20D), with a concomitant increase in circularity index (Fig. 20E). In fact, EHP significantly diminished microglia area to 53.7±4.5% of control ($p<0.01$), affecting also the perimeter that was significantly decreased to 48.7±7.4% of the control ($p<0.001$) and reducing the Ferret's diameter significantly to 64.3±5.8% of the control ($p<0.01$). Additionally, microglia circularity index was significantly increased to 0.36±0.05 by EHP stimulus ($p<0.05$) when compared with control conditions (Fig. 20E). Furthermore, the blockade of the $A_{2A}R$ partially prevented the effect of EHP by significantly increasing the area to 91.4±11.1% of control ($p<0.01$) when compared to EHP conditions, as well as perimeter to 87.1±20.4% of control and Ferret's diameter that increased to 90.5±7.2% of control. Microglial circularity index was not different from control conditions showing the partial prevention of $A_{2A}R$ blockade in EHP induced microglia morphology.

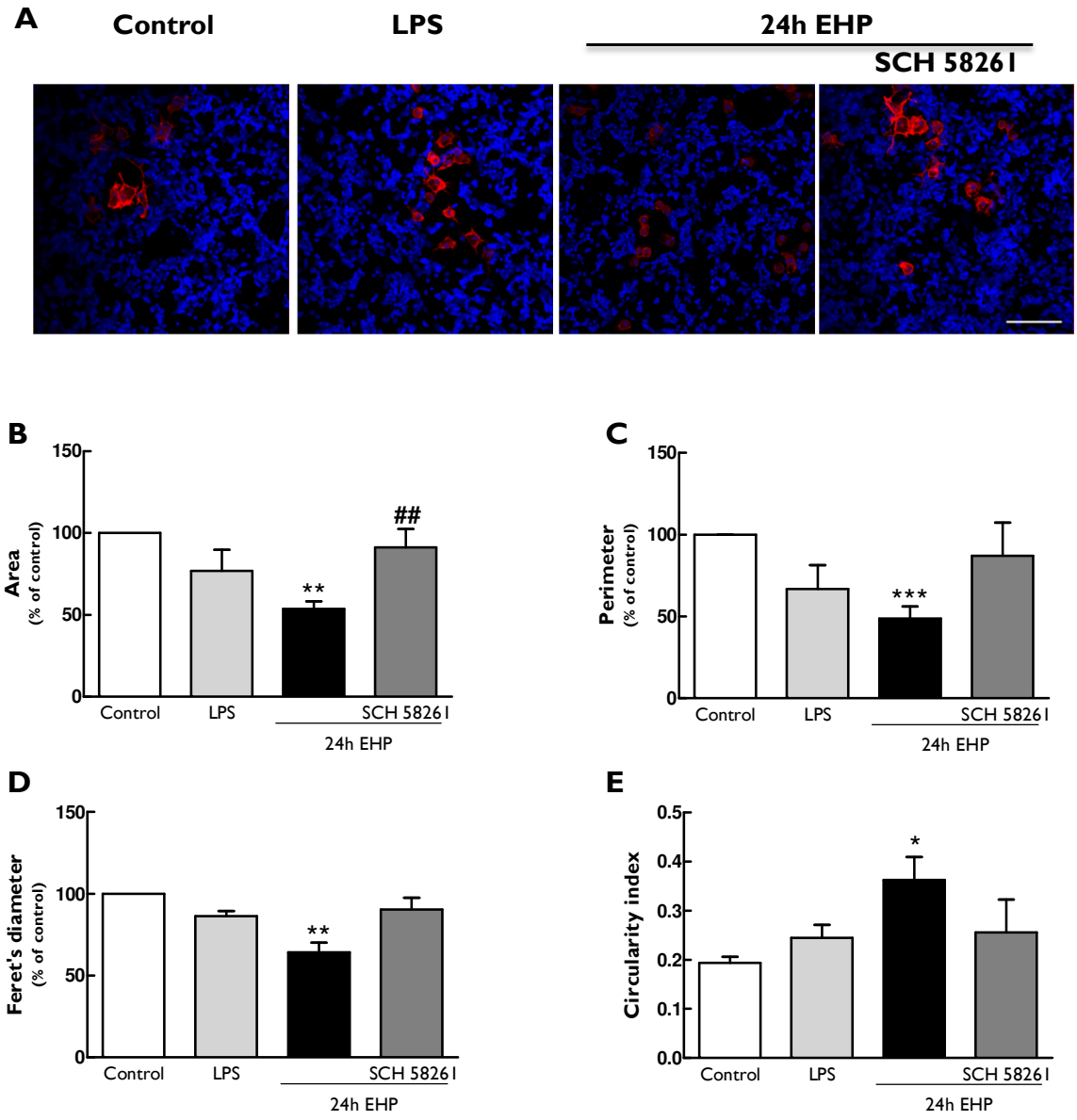

Figure 20 - Elevated hydrostatic pressure changes microglia morphology. Primary mixed retinal cell cultures were pre-treated with 50 nM SCH 58261, followed by 1 µg/ml LPS or EHP for 24 hours. Microglial cells were identified by immunocytochemistry with anti-CD11b (red). Nuclei were counterstained with DAPI (blue). Representative images are depicted in **A**. Microglia area (**B**), perimeter (**C**), Feret's diameter (**D**), and circularity index (**E**) were determined using ImageJ. The results are expressed as percentage of control, from 3 to 6 independent experiments, performed in duplicate. *p<0.05, **p<0.01, ***p<0.001, compared with control; #p<0.05, compared with EHP, Kruskall-Wallis test, followed by Dunn's multiple comparison test. Bar: 100 µm.

Table 1 – Morphological parameters in control cells.

	Area (µm^2)	Perimeter (µm)	Feret's diameter (µm)	Circularity index
Control	955.0±248.8	342.9±52.8	62.4±9.3	0.19±0.01

3.6. Elevated hydrostatic pressure increases the number of microglia in primary mixed retinal neural cell cultures

We observed that the number of microglia in primary retinal neural cell cultures exposed to EHP for 24h significantly increased (Fig. 21A and B), suggesting that microglia might be proliferating in response to EHP.

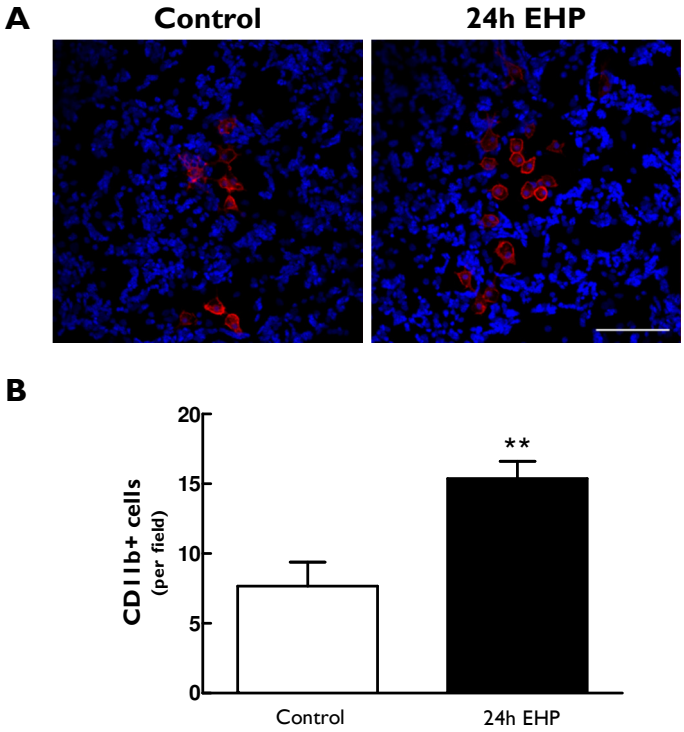

Figure 21- Elevated hydrostatic pressure increases the number of microglia in primary mixed retinal neural cell cultures. Primary mixed retinal cultures where challenged with EHP for 24 hours. Microglial cells were identified by immunocytochemistry with anti-CD11b (red). Nuclei were counterstained with DAPI (blue). Representative images are depicted in **A**. (**B**) The number of CD11b-immunoreactive per field was counted in 7 independent experiments, performed in duplicate. **p<0.01, Mann-Whitney test. Bar: 100 μm.

In order to assess if the increase in microglia cell number was due to cell proliferation, we performed a proliferation assay by incubating the cells with a nuclear marker of cell division. Cell cultures were incubated with EdU, an analog of thymidine that intercalates in the DNA during S phase (Salic and Mitchison, 2008). Primary retinal neural cell cultures were pre-treated with 50 nM SCH 58261 and subjected to EHP for 24 hours to evaluate the effect of EHP and $A_{2A}R$ blockade in cell proliferation. In control, 35.5±5.4 cells were stained with EdU, indicating that cells proliferate in control conditions. LPS increased the number of the EdU+ cells to 124.8±26.5% of control (Fig. 22A).

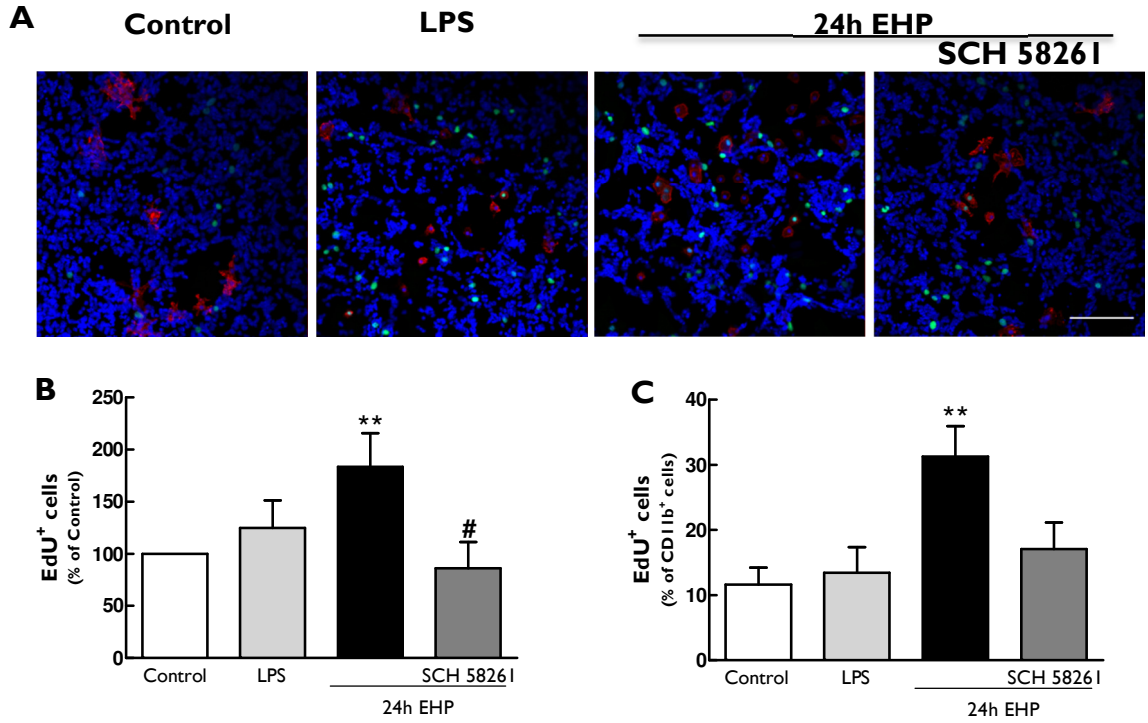

Figure 22 – $A_{2A}R$ blockade prevents cell proliferation induced by elevated hydrostatic pressure in retinal primary mixed retinal cultures. Primary mixed retinal cultures were pre-treated with 50 nM SCH 58261, followed by 1 µg/ml LPS or EHP for 24 hours. Cell proliferation was measured by counting the number of EdU^+ cells (green). (**A**) Microglial cells were labeled by immunocytochemistry with an antibody anti-CD11b (red). Nuclei were counterstained with DAPI (blue) Representative images are depicted. (**B**) The number of cells stained with EdU (EdU^+) per field was counted and the results are expressed as percentage of control. (**C**) The number of microglia cells proliferating (EdU^+-CD11b-immunoreactive cells) was counted and expressed as the ratio $EdU^+CD11b^+/CD11b^+$, from 5 independent experiments, performed in duplicate. #p<0.05 compared to EHP, **p<0.01 compared to control, Kruskall-Wallis test, followed by Dunn's multiple comparison test. Bar: 100 µm.

In addition, the exposure of primary retinal neural cell cultures to EHP for 24h significant increased the number of EDU^+ cells to 183.7±32.3% of control (p<0.01). The treatment with $A_{2A}R$ antagonist significantly prevented cell proliferation induced by EHP (86.2±25.1% of control, p<0.05) (Fig. 22B).

We also evaluated if microglia cells were proliferating by counting the number of proliferating (EdU^+) microglia cells ($CD11b^+$) (Fig. 22C). In control conditions only 11.7±2.6 of the $CD11b^+$ cells were proliferating whereas the exposure to EHP for 24h lead to a 3-fold (p<0.01) increase in microglia cell proliferation (31.3±4.7 cells). The proliferation of microglia treated with $A_{2A}R$ antagonist following EHP was not different from control conditions (17.1±4.1 cells).

To better clarify the effects of the exposure to EHP in microglia, we used BV-2 cells which is a brain derived microglia cell line.

3.7. Effect of elevated hydrostatic pressure on the levels of pro-inflammatory cytokines in BV-2 cells

To assess the effect of the exposure to EHP the release of IL-1β and TNF were quantified by ELISA in BV-2 culture medium. In control conditions, the levels of IL-1β were 10.1±4.8 pg/ml. As expected, LPS increased the extracellular levels of IL-1β to 21.6±6.9 pg/ml. Furthermore, when the cells were exposed to EHP for 4 hours or 24 hours the levels of IL-1β were 31.9±3.0 pg/ml and 28.3±1.6 pg/ml, respectively (Fig. 23A).

The levels of TNF in control conditions were 17.6±3.8 pg/ml (Fig. 23B). Incubation with LPS increased TNF concentration in culture medium to 778.3±118.4 pg/ml. When the cells were exposed to EHP for 4h or 24h, TNF levels were 25.8±1.5 pg/ml and 26.2±3.8 pg/ml, respectively.

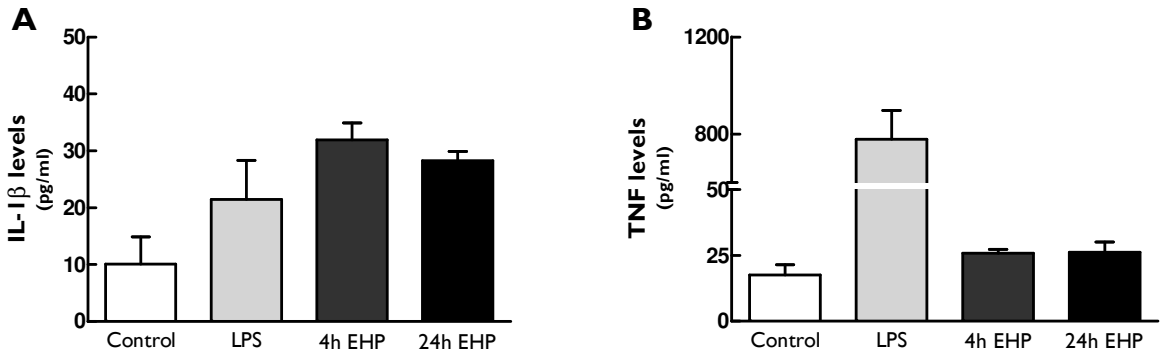

Figure 23 - **Effect of elevated hydrostatic pressure on the levels of pro-inflammatory cytokines in BV-2 cells.** BV-2 cells were challenged with 100 ng/ml LPS or EHP for 4 or 24 hours. Extracellular levels of IL-1β (**A**) and TNF (**B**) were quantified by ELISA in cell culture medium supernatants. Results are expressed in pg/ml, from 3 to 5 independent experiments performed in duplicate. **p<0.01, Kruskall-Wallis test, followed by Dunn's multiple comparison test.

3.8. Elevated hydrostatic pressure increases BV-2 cell motility

In order to evaluate whether EHP changes the motility of microglia cells, BV-2 cell cultures were exposed to EHP for 4h. The scratch wound assay (Fig. 24A) was used to assess BV-2 cell migration after 4h exposure to EHP. The number of cells in the wound significantly increased when the cells were exposed to EHP (49.9±8.9 cells in control vs 94.4±7.5 cells in EHP; Fig. 24B).

Furthermore, BV-2 cell migration following EHP was assessed using a modified Boyden chamber assay. In addition, the effect mediated by the blockade of $A_{2A}R$ was also evaluated.

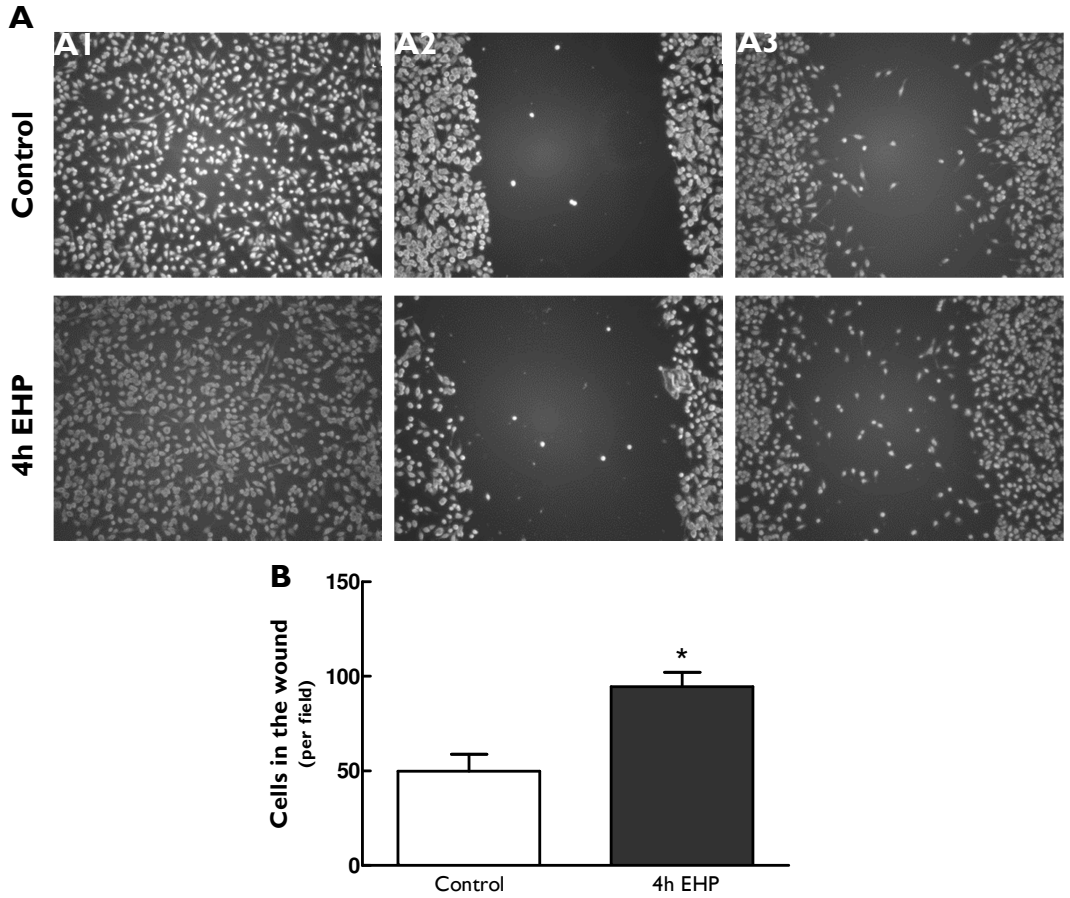

Figure 24 - Elevated hydrostatic pressure increases BV-2 cell motility. BV-2 cells migration was assessed by scratch wound assay (A) Representative images are depicted for the scratch wound assay: immediately before the assay (A1), immediately after the scratch (A2), and at the end of the experiment (A3). (B) The number of cells in the wound was counted per field obtained from 5 independent experiments. *p<0.05, compared with control, Mann-Whitney test.

In control conditions, 33.2 ±11.2 cells per field were counted in the bottom side of the transmembrane insert. When the cells were exposed to EHP, the number of cells in the bottom side of the transwell significantly increased to 254.7±24.5% of control ($p<0.01$) (Fig. 25A). The effect of EHP in microglia migration was totally prevented by $A_{2A}R$ blockade ($p<0.05$) (Fig. 25B).

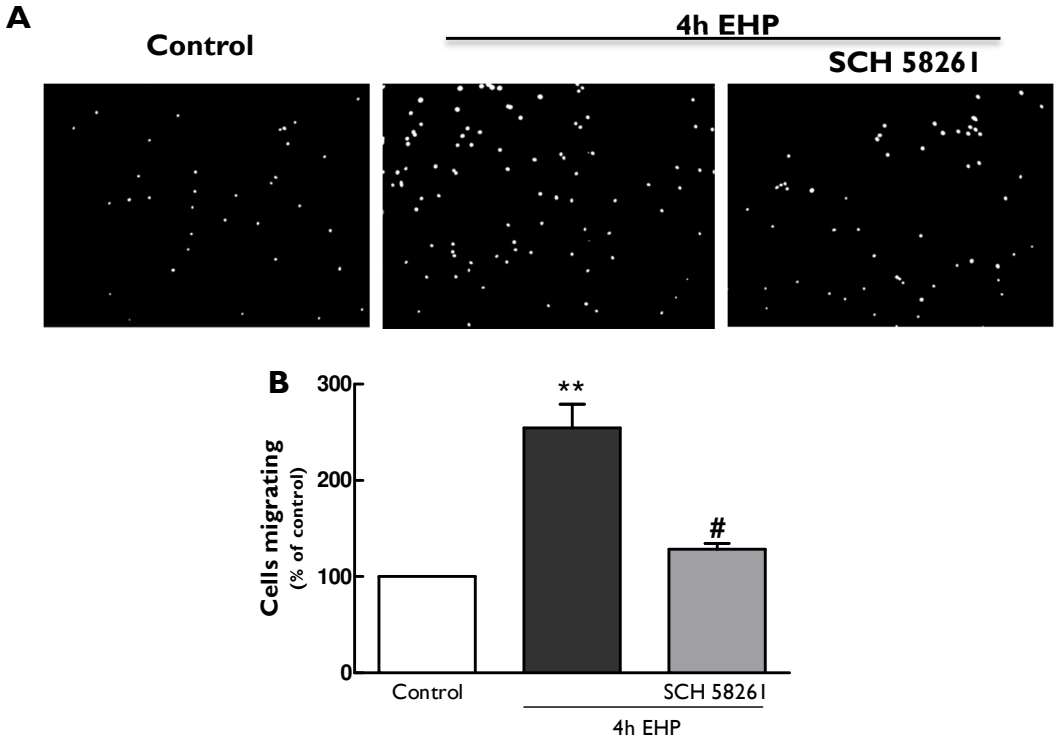

Figure 25 - $A_{2A}R$ blockade prevented elevated hydrostatic pressure induced BV-2 cell motility. Boyden chamber migration assay (A). The number of BV-2 cells in the bottom surface of the transwell was counted.(B) The results expressed as percentage of control, from 4 to 5 independent experiments. *p<0.05, **p<0.01, Kruskall-Wallis test, followed by Dunn's multiple comparison test.

3.9. Effect of elevated hydrostatic pressure on the extracellular levels of ATP and adenosine

An increase in ATP release has been described as one of the mechanistic alterations in neurodegenerative diseases, namely glaucoma (Davalos et al., 2005; Lee, 2013; Reigada et al., 2008). In addition, it is known that the sustained augment in adenosine release or accumulation is a recognized feature of inflammatory conditions (Hasko et al., 2008). Therefore, we evaluated the levels of extracellular ATP and adenosine in BV-2 cell cultures exposed to EHP and studied whether $A_{2A}R$ blockade could affect the levels of ATP or adenosine when the cells are exposed to EHP. Extracellular levels of ATP were quantified by luciferin-luciferase bioluminescence assay in BV-2 cell medium (Fig. 26A). In control, conditions the levels of extracellular ATP were 0.59±0.2 pmol/µg of protein. LPS increased the extracellular ATP levels to 146.3±28.4% of control. Cultures exposed to EHP for 4h or 24h have increased extracellular ATP levels (267.6±82.7% and of 217.5±57.3% of control, respectively). Interestingly, pre-treatment with $A_{2A}R$ antagonist significantly increased the extracellular ATP concentration at both time points studied

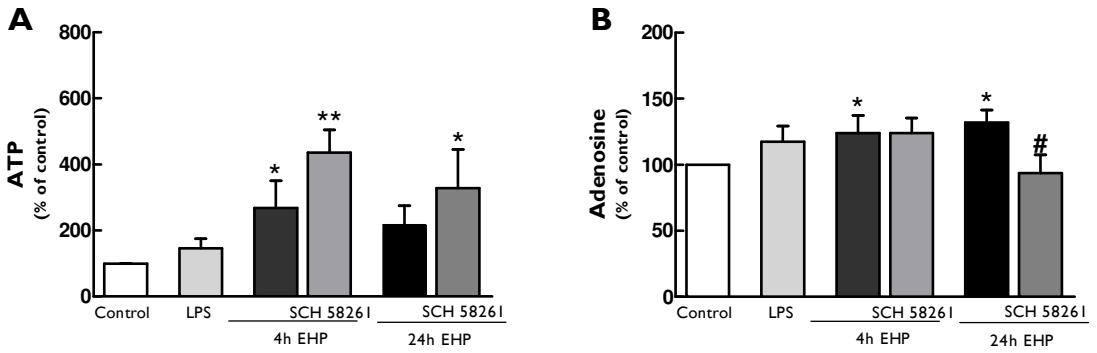

Figure 26 – Effect of elevated hydrostatic pressure on the extracellular levels of ATP and adenosine. BV-2 cells where pre-treated with 50 nM SCH 58261 followed by 100 ng/ml LPS or EHP for 4 hours or 24 hours. (**A**) Extracellular ATP was quantified by luciferin-luciferase bioluminescence assay in cell culture medium. The results were normalized to the concentration of protein and are expressed as percentage of control, from 4 to 5 independent experiments. (**B**) Extracellular adenosine was quantified by HPLC in cell culture medium supernatant. Results were normalized to the amount of protein and are expressed as percentage of control, from 5 to 7 independent experiments. *p<0.05, compared to control #p<0.01, compared to 24H EHP, Kruskall-Wallis test, followed by Dunn's multiple comparison test.

(435.5±68.9% of control and 328.6±117.2% of control, for 4h and 24 h with EHP, respectively).

The levels of extracellular adenosine were quantified by HPLC (Fig. 26B). Adenosine levels in control conditions were 0.81±0.17 pmol/µg of protein and increased to 124.15±13.22% of control and to 131.9±9.6% of control after 4h and 24h exposure to EHP, respectively. The pre-treatment with $A_{2A}R$ antagonist did not change adenosine levels when the cells were exposed to EHP for 4 hours (124.0±11.3% of control) but significantly decreased adenosine concentration at 24 hours (78.2±13.9% of control; p<0.05).

3.10. Phagocytosis increases upon elevated hydrostatic pressure in BV-2 cells and is prevented by the blockade of $A_{2A}R$

The phagocytic efficiency of BV-2 cells was evaluated following exposure to EHP for 24h. The effect of $A_{2A}R$ blockade in the phagocytosis induced by EHP was also assessed. In other to allow the visibility of BV-2 cell engulfment, fluorescent latex beads were incubated 1h before the end of the experiment. BV-2 cells where stained with phalloidin that binds to F-actin, allowing cell visualization. In control conditions, most of the cells did not have beads incorporated (Fig. 27A).

Incubation with LPS increased the number of beads incorporated and the number of cells with beads (Fig. 27A). Exposure to EHP significantly increased phagocytic efficiency (22.5±2.4%) when compared with control conditions (p<0.01). Pre-treatment with $A_{2A}R$

antagonist significantly prevented the increase in phagocytic efficiency induced by EHP exposure ($p<0.01$) (Fig. 27B).

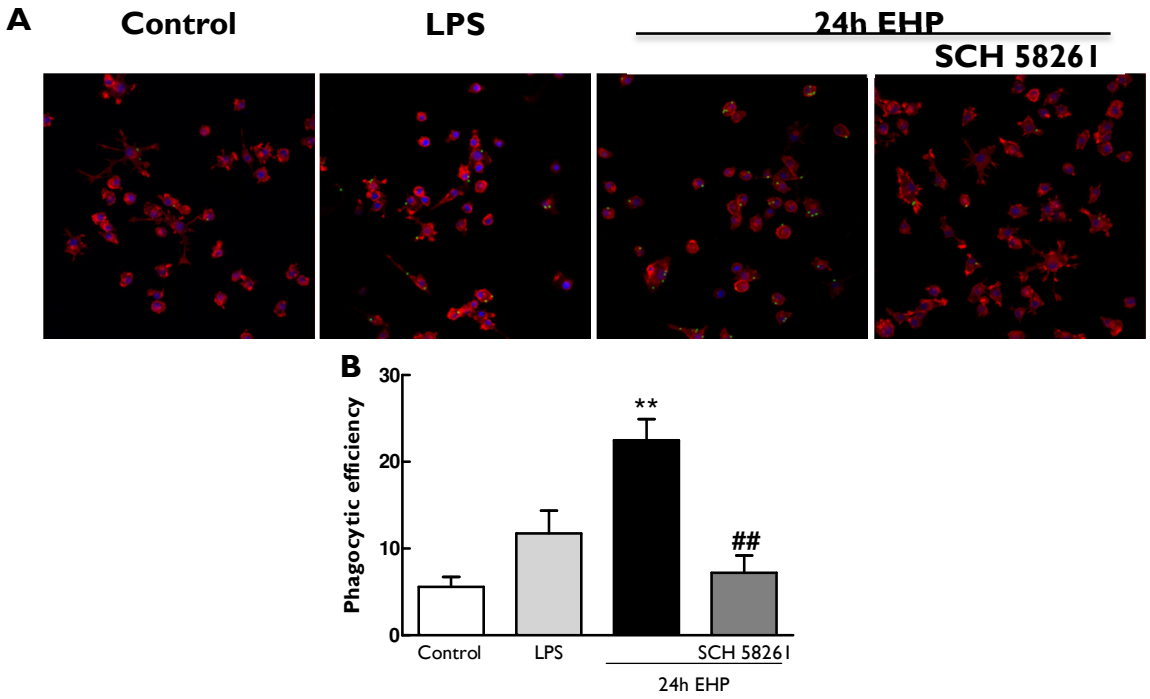

Figure 27 - Phagocytic efficiency of BV-2 cell line is increased after exposure to elevated hydrostatic pressure and is prevented by the blockade of A2AR. BV-2 cell cultures where pre-treated with 50 nM SCH 58261 followed by 100 ng/ml LPS or EHP for 24 hours. Phagocytosis was assessed with fluorescent beads. (A) Representative images of BV-2 cells stained with phalloidin (red) with incorporated beads (green). Nuclei were counterstained with DAPI (blue). (B) Phagocytic efficiency calculated from 4 to 6 independent experiments, performed in duplicate. #$p<0.05$ compared to EHP, **$p<0.01$ compared to control, Kruskall-Wallis test, followed by Dunn's multiple comparison test.

3.11. Effect of elevated hydrostatic pressure on the morphology of microglia in retinal organotypic cultures

To assess the effects of EHP in a more complex model and to investigate the potential of the $A_{2A}R$ to modulate these alterations, retinal explants were obtained from $A_{2A}R$-KO mice and wild type mice.

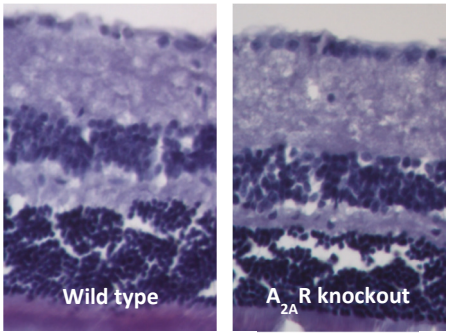

Figure 28 - **Retinal structure in WT and KO-$A_{2A}R$ mice.** Retinal sections were stained with hematoxylin and eosin and the preparations were observed in a light microscope (Leica DM 4000 B). Representative images are depicted.

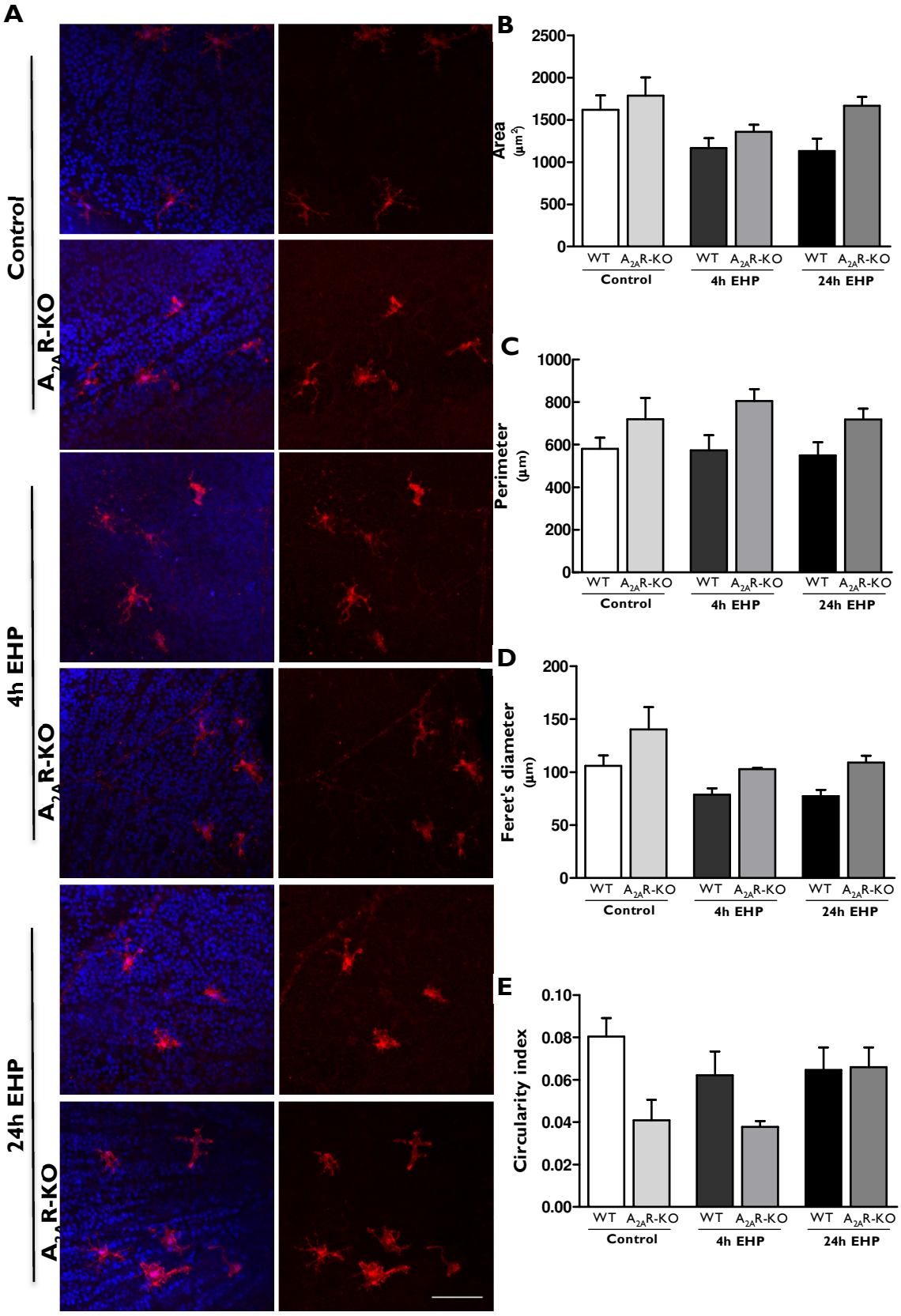

Figure 29 – Effect of elevated hydrostatic pressure on the morphology of microglia in retinal organotypic cultures. Organotypic retinal cultures were exposed to EHP for 4 or 24 h. Explants were both obtained from wild type and KO-A2AR mice. Microglial cells were identified by immunocytochemistry with anti-Iba-1 (red). Nuclei were counterstained with DAPI (blue). Representative images are depicted in A. Changes in cell morphology were quantified using imageJ according to area (B), perimeter (C), Feret's diameter (D), and circularity (E). Results from 2 independent experiments. Bar: 100 µm.

Retinal thickness is similar between wild type and A_{2A}R-KO mice indicating no major differences in retinal structure between the two groups. Organotypic retinal cultures obtained from wild type and A_{2A}R-KO mice were exposed to EHP for 4h or 24h and microglia were stained with an antibody anti Iba-1, We did not observe significant alterations in the morphology of microglia after 4h and 24h of EHP (Fig. 29A). Some alterations were observed between WT and A_{2A}R-KO mice (Fig. 29B) but these results are preliminary (n=2) and therefore we did not assess statistical inference.

Chapter 4

Discussion

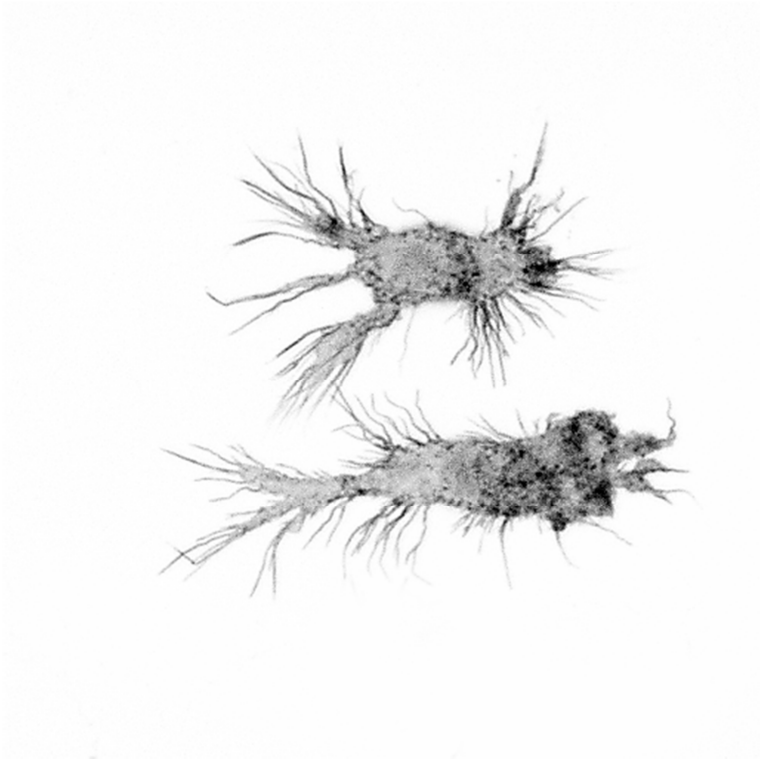

"Microglia – BV-2 cell line"

4. Discussion

Glaucoma is the second leading cause of visual loss worldwide and is expected that by the year 2020 approximately 80 million people will suffer from this disease (Quigley and Broman, 2006). Characterized by RGC death and damage to the optic nerve, glaucoma is a neurodegenerative disease that leads to progressive and irreversible vision loss (Almasieh et al., 2012; Quigley, 1999). The main risk factor for the development of glaucoma is elevated IOP. Current treatments are focused on lowering IOP but patients continue to lose vision despite IOP control (Cheung et al., 2008). Therefore, new and more effective treatments are necessary, and neuroprotection of RGCs is considered to offer potential as an alternative therapy (Cordeiro and Levin, 2011).

Several experimental models have been developed based on elevated IOP, allowing the study of the molecular mechanisms underlying glaucomatous alterations. These include animal models like retinal ischemia-reperfusion injury (Johnson and Tomarev, 2010; Selles-Navarro et al., 1996) and obstruction of trabecular meshwork or episcleral veins (Almasieh et al., 2012; Urcola et al., 2006) as well as *in vitro* models in which cells are exposed to EHP (Agar et al., 2006; Reigada et al., 2008; Sappington et al., 2006; Zeiss, 2013). Herein, we studied the role of $A_{2A}R$ on microglia-mediated inflammation triggered by EHP, as an *in vitro* model of elevated IOP.

Neuroinflammation has been described as an important player in the pathogenesis of glaucoma, namely contributing to RGC death (Vohra et al., 2013). Microglia activation has an important role in neuroinflammation (Block and Hong, 2005; Lee, 2013), and it may contribute for the pathophysiology of glaucoma (Almasieh et al., 2012; Chua et al., 2012; Lee, 2013). In retinal neural cell cultures, EHP exposure increased the release of NO. The retinal cell culture is composed of neurons, Müller cells, astrocytes and microglia (Alvaro et al., 2007; Santiago et al., 2006). All these cells may express iNOS and release NO (Farina et al., 2007; Lee, 2013; Newman and Reichenbach, 1996). Nevertheless, in our conditions, after EHP, iNOS was detected in microglia, suggesting these cells are the main producers of NO upon an increase in EHP. The mechanisms underlying microglia activation in glaucomatous optic neuropathy are not clarified yet. Although, in models of neurodegenerative diseases, the increased production and release of ROS has been described as an early event further triggering microglia activation and release of pro-inflammatory cytokines (Block and Hong, 2005). In our experimental conditions, EHP altered the expression and release of pro-inflammatory mediators in retinal neural cell

cultures and in the BV-2 cell line, suggesting that microglia are contributing to the inflammatory milieu in these conditions.

In the resting state, microglia cells are ramified, evenly distributed, and constantly surveying the parenchyma. Upon activation, microglia change their morphology becoming more amoeboid and less ramified (Kettenmann et al., 2011; Kreutzberg, 1996; Lee, 2013). In retinal neural cell cultures, the morphology of microglia, upon exposure to EHP, shifted from ramified to more amoeboid, consistent with an activated phenotype.

Previous studies describe microglia inflammatory responses as being initially protective, although sustained and exacerbated responses may ultimately lead to cell loss (Karlstetter et al., 2010). The exposure of retinal neural cultures to EHP markedly increased cell death. It remains to be clarified whether EHP-induced cell death triggered microglia activation or EHP directly elicited a microglia pro-inflammatory response leading to cell death. We can not discard the direct impact of EHP on neural cell loss, although the experiments performed with the microglia cell line suggest that EHP elicits a pro-inflammatory response that would potentially damage cells. Nevertheless, EHP per se can induce apoptosis in neuronal cell lines (Agar et al., 2006; Agar et al., 2000). One of the functions of microglia is to phagocyte damaged cells, cell debris and pathogens (Kettenmann et al., 2011; Langmann, 2007; Petersen and Dailey, 2004). We observed a clear increase in microglia with engulfed dead cells (TUNEL+ cells), either due to an increase in the number of dead cells that needed to be removed or to an increased phagocytosis elicited by EHP, as we observed with the BV-2 cell line.

Microglial cells are also known for promptly migrate to the site of lesion and proliferate (Kettenmann et al., 2011). We found that the motility and proliferation of microglia increased after exposure to EHP. In addition, cells other than microglia are also proliferating. Evidence indicates that astrocytes and Müller cells also play an important role in neuroinflammatory responses and that pro-inflammatory mediators highly increase their proliferation (Dyer and Cepko, 2000; Farina et al., 2007). Therefore, since these cells are also present, we can not rule out their contribution to the inflammatory milieu nor as putative proliferating cells. In addition, retinal neuronal progenitor cells have also been identified in these cultures (Alvaro et al., 2008) and may also be proliferating accounting for the observed results.

The extracellular levels of ATP increased in BV-2 cells upon exposure to EHP. Others have demonstrated that extracellular ATP levels increase in the retina upon

pressure elevation (Reigada et al., 2008; Resta et al., 2007). Interestingly, the levels of ATP are elevated in the anterior chamber of glaucomatous patients (Li et al., 2011; Zhang et al., 2007). The mechanisms by which ATP is released from microglia were not addressed in this work, although several mechanisms have been proposed, namely through vesicular nucleotide transporter-dependent exocytosis (Imura et al., 2013) and lysosomal exocytosis (Dou et al., 2012). In addition, exposure of bovine eyecup preparations to elevated pressure increases extracellular ATP levels in which pannexin hemichannels have a role (Reigada et al., 2008). In line with the findings of microglial released ATP, it has been described that, in activated microglia, ATP induces process retraction leading to a more amoeboid morphology and triggering cell migration (Davalos et al., 2005; Gyoneva et al., 2009; Imura et al., 2013; Kettenmann et al., 2011), which could explain the observed changes in microglia morphology and increased motility induced by EHP.

Adenosine can be formed extracellularly through ATP catabolism (reviewed in (Cunha, 2001) by ectoenzymes (Fredholm et al., 2001). We found an increase in extracellular adenosine upon EHP in BV-2 cell line, which is in agreement with the increased ATP levels. Microglial cell function is modulated by extracellular adenosine through interaction with ARs (Zhong et al., 2013). Activation of A_{2A}Rs in microglia has been shown to stimulate the proliferation of these cells and to upregulate cyclooxygenase-2 expression, resulting in inflammation (Abbracchio and Cattabeni, 1999). In addition, the pharmacological blockade or the genetic inactivation of A_{2A}R has been described to afford robust neuroprotection against several noxious conditions, namely in models of cerebral ischemia, Parkinson's, Alzheimer's and Huntington's diseases (Gomes et al., 2011), probably through the control of microglia reactivity (Dare et al., 2007). In the retina, A_{2A}R can be detected in INL and GCL, with minor expression in the ONL (Kvanta et al., 1997). It is also present in retinal neural cell cultures (Vindeirinho et al., 2013) In previous studies A_{2A}R expression has been reported to increase in response to noxious and inflammatory stimulus (Cunha, 2005; Vindeirinho et al., 2013; Wittendorp et al., 2004). Although we were not able to detect changes concerning A_{2A}R expression between control and EHP conditions (due to the variability of the results), retinal microglial cells express A_{2A}R (Liou et al., 2008) and previous results obtained in our laboratory have demonstrated that A_{2A}R density and expression increase upon LPS in microglia(Madeira et al., 2012).

In our study, we found that the blockade of $A_{2A}R$ prevented the increase in cell death induced by EHP. The protective effects of $A_{2A}R$ blockade have been demonstrated previously in different models of degenerative diseases (Abbracchio and Cattabeni, 1999; Cunha, 2005; Rebola et al., 2011). Furthermore, $A_{2A}R$ blockade decreased EHP-induced NO release and iNOS expression and immunoreactivity. In purified retinal microglia cells, the blockade of $A_{2A}R$ has been demonstrated to prevent the increase in NO release induced by LPS (Madeira et al., 2012), further supporting the contribution microglia to the production of NO and the role exerted by $A_{2A}R$.

In addition to the effects of $A_{2A}R$ blockade on decreasing EHP-induced cell death, the $A_{2A}R$ antagonist also decreased the number of microglia with engulfed dead cells. In line with this finding, EHP-induced microglia phagocytosis in BV-2 cells was prevented by $A_{2A}R$ blockade. It has already been reported that $A_{2A}R$ blockade prevents LPS-induced microglia phagocytosis in purified retinal microglial cell cultures (Madeira et al., 2012). These results indicate that either the blockade of A2AR decreases cell death thereby reducing the engulfment of dead cells by microglia, or the blockade of the receptor halts microglia activation, thus preventing phagocytosis.

The blockade of $A_{2A}R$ was able to decrease the EHP-induced retraction of microglia processes in mixed cultures. The dynamics of microglia processes are under the control of $A_{2A}R$ both in physiological and pathological conditions (Orr et al., 2009). Furthermore, the treatment with SCH 58261 prevented the EHP-induced microglia cell motility, possibly by preventing its activation. Additionally, microglia proliferation induced by EHP was clearly reduced by the blockade of $A_{2A}R$. In fact, blockade of A_1R or $A_{2A}R$ has been described to prevent microglial cell proliferation (Fiebich et al., 1996; Gebicke-Haerter et al., 1996). Interestingly, the blockade of the $A_{2A}R$ was able to decrease the proliferation of microglia, but also of other cells. Astrocytes are active players in the inflammatory response (Pekny et al., 2014) and the blockade of $A_{2A}R$ has been reported to hamper astrogliosis, thus preventing astrocytic proliferation (Dare et al., 2007). Therefore, we in addition to microglia we could relate the decrease in cell proliferation driven by the $A_{2A}R$ antagonist, to its modulatory effects in astrocytes.

The modulation of $A_{2A}R$ activity in ATP and adenosine levels was also assessed. Extracellular ATP levels where augmented by the blockade of $A_{2A}R$. Extracellular ATP is known to be very instable being quickly converted into adenosine by Ecto-5'NTs and interacting with purinergic receptors (Hasko et al., 2005). Nevertheless, the blockade of

the $A_{2A}R$ diminishes the levels of extracellular adenosine suggesting an effect of $A_{2A}R$ in adenosine turnover or uptake, possible through the impairment of Ecto-5'NT (CD73) activity. In striatal neurons, CD73 has been described to physically interact with $A_{2A}R$ (Augusto et al., 2013). CD73 activity is responsible for the formation of adenosine that activates $A_{2A}R$ (Augusto et al., 2013). In addition, in synapses the activity of nucleoside transporters is controlled by $A_{2A}R$ (Pinto-Duarte et al., 2005).

Taken together, the effects in BV-2 microglia reactivity can be explained by its response to ATP gradients released from damaged cells or in response to EHP mechanical stimulus. ATP is promptly converted into adenosine through ectonucleotidases and consequently activates $A_{2A}R$ in microglia. Once $A_{2A}R$ is blocked, there is a consequent impair in microglia activation and an increase in ATP accumulation that apparently is not converted to adenosine.

The retinal organotypic culture has been described has a suitable model to evaluate cellular and molecular signaling mechanisms and to study neuroprotection (Bull et al., 2011). Therefore this model was used to assess the effects of $A_{2A}R$ genetic knockout upon EHP. We did not observe clear differences in microglia morphology after exposure to EHP. Nevertheless, previous findings in our laboratory demonstrated changes in microglia morphology (to a more amoeboid morphology) in rat retinal explants submitted to EHP. One possible explanation for these discrepancies may be that the species (rat or mouse) might influence the efficiency of the model and thereby we should consider increase the time of exposure and/or the magnitude of pressure. Nevertheless, prior studies in mice retinal explants have shown that microglia motility, thereby activation, increases upon a noxious insult without significant changes in cell ramification (Kettenmann et al., 2011; Lee et al., 2008), demonstrating that evaluation of microglia morphology as the single parameter for microglia activation is limited.

Taken together, the alterations in microglial morphology and in the release of pro-inflammatory mediators indicate that EHP is triggering microglia activation. These results suggest that our experimental model may be a suitable *in vitro* model to study the neuroinflammatory responses of the retina in the context of glaucoma.

In addition, our results indicate that the blockade of the $A_{2A}R$ prevents microglia reactivity which may attenuate the damage caused by EHP. This may have an impact on future studies addressing RGC neuroprotection in the context of glaucoma.

Chapter 5

Concluding remarks and future perspectives

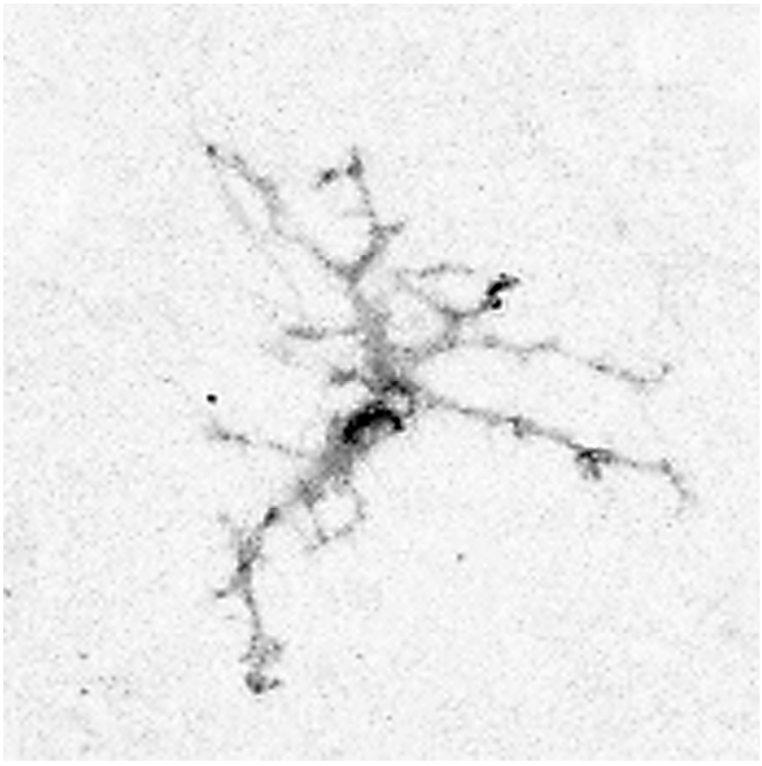

"Microglia cell – Retinal organotypic cell culture"

5. Concluding remarks and future perspectives

The results presented in this thesis allow us to conclude that EHP model mimics the deleterious effects described in glaucomatous patients and experimental models and the blockade of $A_{2A}R$ may prevent neuronal damage by controlling microglia reactivity. In fact we were able to demonstrate that:

- EHP increased oxidative stress in retinal neural cell cultures that was diminished by pre-treatment with the $A_{2A}R$ antagonist;
- Altered the expression and release of pro-inflammatory cytokines in retinal neural cell cultures and BV-2 cells was altered upon exposure to EHP.
- Increased microglia phagocytosis, proliferation and migration that were controlled by the blockade of the $A_{2A}R$;
- EHP promoted a shift in microglia morphology from ramified to amoeboid which was prevented by the blockade of $A_{2A}R$;
- Cell death in retinal neural cell cultures increased upon EHP being prevented by pre-treatment with the $A_{2A}R$ antagonist;
- Extracellular of ATP and adenosine levels increased following the exposure to EHP.

Further experiments will be performed to clarify the role of $A_{2A}R$ on the extracellular levels of ATP and adenosine, namely the expression and activity of CD73 and the transport of adenosine through ENTs. Considering that Müller cells and astrocytes have a role in neuroinflammation, we would like also to assess their response to EHP and study the effects operated by $A_{2A}R$ blockade.

Moreover, we will optimize the conditions of EHP in order to compare microglia responses in mice retinal organotypic cultures prepared from wild type and $A_{2A}R$-KO animals.

Chapter 6

References

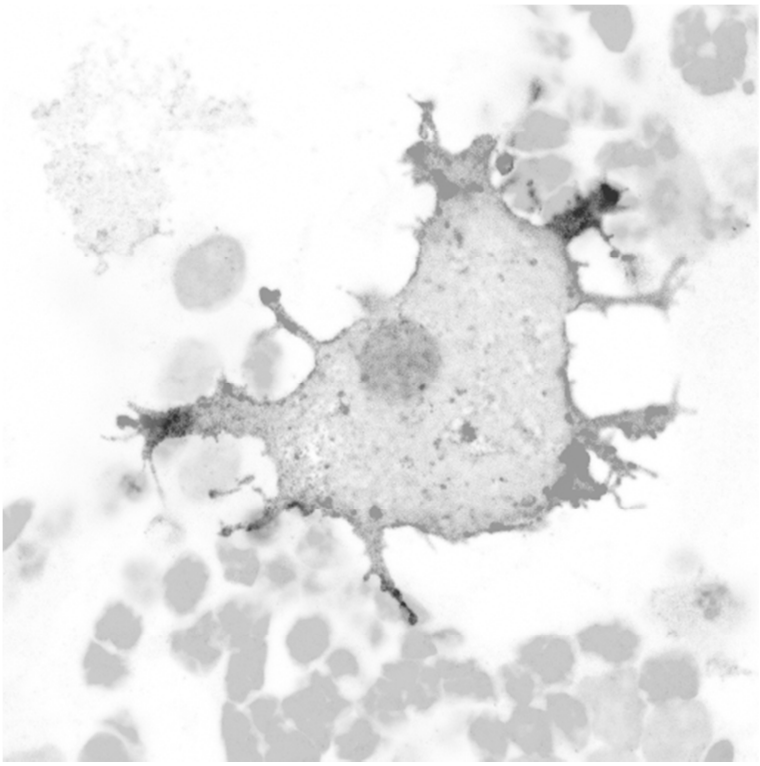

"Microglia cell – Primary mixed neural cell culture"

6. References

Abbracchio, M.P., and Cattabeni, F. (1999). Brain adenosine receptors as targets for therapeutic intervention in neurodegenerative diseases. Annals of the New York Academy of Sciences *890*, 79-92.

Agar, A., Li, S., Agarwal, N., Coroneo, M.T., and Hill, M.A. (2006). Retinal ganglion cell line apoptosis induced by hydrostatic pressure. Brain Res *1086*, 191-200.

Agar, A., Yip, S.S., Hill, M.A., and Coroneo, M.T. (2000). Pressure related apoptosis in neuronal cell lines. J Neurosci Res *60*, 495-503.

Almasieh, M., Wilson, A.M., Morquette, B., Cueva Vargas, J.L., and Di Polo, A. (2012). The molecular basis of retinal ganglion cell death in glaucoma. Progress in retinal and eye research *31*, 152-181.

Alvaro, A.R., Martins, J., Araujo, I.M., Rosmaninho-Salgado, J., Ambrosio, A.F., and Cavadas, C. (2008). Neuropeptide Y stimulates retinal neural cell proliferation--involvement of nitric oxide. J Neurochem *105*, 2501-2510.

Alvaro, A.R., Rosmaninho-Salgado, J., Santiago, A.R., Martins, J., Aveleira, C., Santos, P.F., Pereira, T., Gouveia, D., Carvalho, A.L., Grouzmann, E., *et al.* (2007). NPY in rat retina is present in neurons, in endothelial cells and also in microglial and Muller cells. Neurochem Int *50*, 757-763.

Andersen, C.L., Jensen, J.L., and Orntoft, T.F. (2004). Normalization of real-time quantitative reverse transcription-PCR data: a model-based variance estimation approach to identify genes suited for normalization, applied to bladder and colon cancer data sets. Cancer research *64*, 5245-5250.

Augusto, E., Matos, M., Sevigny, J., El-Tayeb, A., Bynoe, M.S., Muller, C.E., Cunha, R.A., and Chen, J.F. (2013). Ecto-5'-nucleotidase (CD73)-mediated formation of adenosine is critical for the striatal adenosine A2A receptor functions. J Neurosci *33*, 11390-11399.

Blackburn, M.R. (2003). Too much of a good thing: adenosine overload in adenosine-deaminase-deficient mice. Trends in pharmacological sciences *24*, 66-70.

Blazynski, C., Mosinger, J.L., and Cohen, A.I. (1989). Comparison of adenosine uptake and endogenous adenosine-containing cells in mammalian retina. Visual neuroscience *2*, 109-116.

Block, M.L., and Hong, J.S. (2005). Microglia and inflammation-mediated neurodegeneration: multiple triggers with a common mechanism. Progress in neurobiology *76*, 77-98.

Bosco, A., Steele, M.R., and Vetter, M.L. (2011). Early microglia activation in a mouse model of chronic glaucoma. J Comp Neurol *519*, 599-620.

Braas, K.M., Zarbin, M.A., and Snyder, S.H. (1987). Endogenous adenosine and adenosine receptors localized to ganglion cells of the retina. Proc Natl Acad Sci U S A *84*, 3906-3910.

Bull, N.D., Johnson, T.V., Welsapar, G., DeKorver, N.W., Tomarev, S.I., and Martin, K.R. (2011). Use of an adult rat retinal explant model for screening of potential retinal ganglion cell neuroprotective therapies. Invest Ophthalmol Vis Sci *52*, 3309-3320.

Cheung, W., Guo, L., and Cordeiro, M.F. (2008). Neuroprotection in glaucoma: drug-based approaches. Optom Vis Sci *85*, 406-416.

Chua, J., Vania, M., Cheung, C.M., Ang, M., Chee, S.P., Yang, H., Li, J., and Wong, T.T. (2012). Expression profile of inflammatory cytokines in aqueous from glaucomatous eyes. Molecular vision *18*, 431-438.

Cohen, L.P., and Pasquale, L.R. (2014). Clinical Characteristics and Current Treatment of Glaucoma. Cold Spring Harbor perspectives in medicine *4*.

Cordeiro, M.F., and Levin, L.A. (2011). Clinical evidence for neuroprotection in glaucoma. Am J Ophthalmol *152*, 715-716.

Cunha-Vaz, J., Bernardes, R., and Lobo, C. (2011). Blood-retinal barrier. European journal of ophthalmology *21 Suppl 6*, S3-9.

Cunha-Vaz, J.G. (2004). The blood-retinal barriers system. Basic concepts and clinical evaluation. Experimental eye research *78*, 715-721.

Cunha, R.A. (2001). Regulation of the ecto-nucleotidase pathway in rat hippocampal nerve terminals. Neurochemical research *26*, 979-991.

Cunha, R.A. (2005). Neuroprotection by adenosine in the brain: From A(1) receptor activation to A (2A) receptor blockade. Purinergic Signal *1*, 111-134.

Dare, E., Schulte, G., Karovic, O., Hammarberg, C., and Fredholm, B.B. (2007). Modulation of glial cell functions by adenosine receptors. Physiology & behavior *92*, 15-20.

Davalos, D., Grutzendler, J., Yang, G., Kim, J.V., Zuo, Y., Jung, S., Littman, D.R., Dustin, M.L., and Gan, W.B. (2005). ATP mediates rapid microglial response to local brain injury in vivo. Nature neuroscience *8*, 752-758.

de Mendonca, A., Sebastiao, A.M., and Ribeiro, J.A. (2000). Adenosine: does it have a neuroprotective role after all? Brain research Brain research reviews *33*, 258-274.

Dias, R.B., Rombo, D.M., Ribeiro, J.A., Henley, J.M., and Sebastiao, A.M. (2013). Adenosine: setting the stage for plasticity. Trends in neurosciences *36*, 248-257.

Dou, Y., Wu, H.J., Li, H.Q., Qin, S., Wang, Y.E., Li, J., Lou, H.F., Chen, Z., Li, X.M., Luo, Q.M.*, et al.* (2012). Microglial migration mediated by ATP-induced ATP release from lysosomes. Cell research *22*, 1022-1033.

Dyer, M.A., and Cepko, C.L. (2000). Control of Muller glial cell proliferation and activation following retinal injury. Nature neuroscience *3*, 873-880.

Farina, C., Aloisi, F., and Meinl, E. (2007). Astrocytes are active players in cerebral innate immunity. Trends in immunology *28*, 138-145.

Ferrer-Martin, R.M., Martin-Oliva, D., Sierra, A., Carrasco, M.C., Martin-Estebane, M., Calvente, R., Marin-Teva, J.L., Navascues, J., and Cuadros, M.A. (2014). Microglial cells in organotypic cultures of developing and adult mouse retina and their relationship with cell death. Experimental eye research *121*, 42-57.

Fiebich, B.L., Biber, K., Lieb, K., van Calker, D., Berger, M., Bauer, J., and Gebicke-Haerter, P.J. (1996). Cyclooxygenase-2 expression in rat microglia is induced by adenosine A2a-receptors. Glia *18*, 152-160.

Fredholm, B.B., AP, I.J., Jacobson, K.A., Klotz, K.N., and Linden, J. (2001). International Union of Pharmacology. XXV. Nomenclature and classification of adenosine receptors. Pharmacological reviews *53*, 527-552.

Gavet, O., and Pines, J. (2010). Progressive activation of CyclinB1-Cdk1 coordinates entry to mitosis. Developmental cell *18*, 533-543.

Gebicke-Haerter, P.J., Christoffel, F., Timmer, J., Northoff, H., Berger, M., and Van Calker, D. (1996). Both adenosine A1- and A2-receptors are required to stimulate microglial proliferation. Neurochem Int *29*, 37-42.

Gomes, C., Ferreira, R., George, J., Sanches, R., Rodrigues, D.I., Goncalves, N., and Cunha, R.A. (2013). Activation of microglial cells triggers a release of brain-derived neurotrophic factor (BDNF) inducing their proliferation in an adenosine A2A receptor-dependent manner: A2A receptor blockade prevents BDNF release and proliferation of microglia. J Neuroinflammation *10*, 16.

Gomes, C.V., Kaster, M.P., Tome, A.R., Agostinho, P.M., and Cunha, R.A. (2011). Adenosine receptors and brain diseases: neuroprotection and neurodegeneration. Biochim Biophys Acta *1808*, 1380-1399.

Gomez-Nicola, D., Fransen, N.L., Suzzi, S., and Perry, V.H. (2013). Regulation of microglial proliferation during chronic neurodegeneration. J Neurosci *33*, 2481-2493.

Gupta, N., Brown, K.E., and Milam, A.H. (2003). Activated microglia in human retinitis pigmentosa, late-onset retinal degeneration, and age-related macular degeneration. Experimental eye research *76*, 463-471.

Gyoneva, S., Orr, A.G., and Traynelis, S.F. (2009). Differential regulation of microglial motility by ATP/ADP and adenosine. Parkinsonism & related disorders *15 Suppl 3*, S195-199.

Hasko, G., Linden, J., Cronstein, B., and Pacher, P. (2008). Adenosine receptors: therapeutic aspects for inflammatory and immune diseases. Nat Rev Drug Discov *7*, 759-770.

Hasko, G., Pacher, P., Vizi, E.S., and Illes, P. (2005). Adenosine receptor signaling in the brain immune system. Trends in pharmacological sciences *26*, 511-516.

Hines, D.J., Choi, H.B., Hines, R.M., Phillips, A.G., and MacVicar, B.A. (2013). Prevention of LPS-induced microglia activation, cytokine production and sickness behavior with TLR4 receptor interfering peptides. PLoS ONE *8*, e60388.

Hosoya, K.-i., and Tomi, M. (2008). Inner Blood—Retinal Barrier: Transport Biology and Methodology. In Drug Absorption Studies, C. Ehrhardt, and K.-J. Kim, eds. (Springer US), pp. 321-338.

Imura, Y., Morizawa, Y., Komatsu, R., Shibata, K., Shinozaki, Y., Kasai, H., Moriishi, K., Moriyama, Y., and Koizumi, S. (2013). Microglia release ATP by exocytosis. Glia *61*, 1320-1330.

Ishikawa, M. (2013). Abnormalities in Glutamate Metabolism and Excitotoxicity in the Retinal Diseases. Scientifica *2013*, 528940.

Ishikawa, M., Yoshitomi, T., Zorumski, C.F., and Izumi, Y. (2010). Effects of acutely elevated hydrostatic pressure in a rat ex vivo retinal preparation. Invest Ophthalmol Vis Sci *51*, 6414-6423.

Ishikawa, M., Yoshitomi, T., Zorumski, C.F., and Izumi, Y. (2011). Downregulation of glutamine synthetase via GLAST suppression induces retinal axonal swelling in a rat ex vivo hydrostatic pressure model. Invest Ophthalmol Vis Sci *52*, 6604-6616.

Johnson, T.V., and Tomarev, S.I. (2010). Rodent models of glaucoma. Brain research bulletin *81*, 349-358.

Jonas, R.A., Yuan, T.F., Liang, Y.X., Jonas, J.B., Tay, D.K., and Ellis-Behnke, R.G. (2012). The spider effect: morphological and orienting classification of microglia in response to stimuli in vivo. PLoS ONE *7*, e30763.

Jones, L.L., Banati, R.B., Graeber, M.B., Bonfanti, L., Raivich, G., and Kreutzberg, G.W. (1997). Population control of microglia: does apoptosis play a role? Journal of neurocytology *26*, 755-770.

Ju, W.K., Kim, K.Y., Lindsey, J.D., Angert, M., Patel, A., Scott, R.T., Liu, Q., Crowston, J.G., Ellisman, M.H., Perkins, G.A., *et al.* (2009). Elevated hydrostatic pressure triggers release of OPA1 and cytochrome C, and induces apoptotic cell death in differentiated RGC-5 cells. Molecular vision *15*, 120-134.

Kaneda, M. (2013). Signal processing in the mammalian retina. Journal of Nippon Medical School = Nippon Ika Daigaku zasshi *80*, 16-24.

Karlstetter, M., Ebert, S., and Langmann, T. (2010). Microglia in the healthy and degenerating retina: insights from novel mouse models. Immunobiology *215*, 685-691.

Kettenmann, H., Hanisch, U.K., Noda, M., and Verkhratsky, A. (2011). Physiology of microglia. Physiological reviews *91*, 461-553.

Kierdorf, K., and Prinz, M. (2013). Factors regulating microglia activation. Front Cell Neurosci *7*, 44.

Klaassen, I., Van Noorden, C.J., and Schlingemann, R.O. (2013). Molecular basis of the inner blood-retinal barrier and its breakdown in diabetic macular edema and other pathological conditions. Progress in retinal and eye research *34*, 19-48.

Kolb, H., Fernandez, E., and Nelson, R. (1995). Webvision: The Organization of the Retina and Visual System. In Webvision: The Organization of the Retina and Visual System, H. Kolb, E. Fernandez, and R. Nelson, eds. (Salt Lake City (UT)).

Kreutzberg, G.W. (1996). Microglia: a sensor for pathological events in the CNS. Trends in neurosciences *19*, 312-318.

Kumar, J.P. (2001). Signalling pathways in Drosophila and vertebrate retinal development. Nature reviews Genetics *2*, 846-857.

Kurpius, D., Wilson, N., Fuller, L., Hoffman, A., and Dailey, M.E. (2006). Early activation, motility, and homing of neonatal microglia to injured neurons does not require protein synthesis. Glia *54*, 58-70.

Kvanta, A., Seregard, S., Sejersen, S., Kull, B., and Fredholm, B.B. (1997). Localization of adenosine receptor messenger RNAs in the rat eye. Experimental eye research *65*, 595-602.

Langmann, T. (2007). Microglia activation in retinal degeneration. J Leukoc Biol *81*, 1345-1351.

Leal, E.C., Santiago, A.R., and Ambrosio, A.F. (2005). Old and new drug targets in diabetic retinopathy: from biochemical changes to inflammation and neurodegeneration. Current drug targets CNS and neurological disorders *4*, 421-434.

Lee, J.E., Liang, K.J., Fariss, R.N., and Wong, W.T. (2008). Ex vivo dynamic imaging of retinal microglia using time-lapse confocal microscopy. Invest Ophthalmol Vis Sci *49*, 4169-4176.

Lee, M. (2013). Neurotransmitters and microglial-mediated neuroinflammation. Current protein & peptide science *14*, 21-32.

Li, A., Zhang, X., Zheng, D., Ge, J., Laties, A.M., and Mitchell, C.H. (2011). Sustained elevation of extracellular ATP in aqueous humor from humans with primary chronic angle-closure glaucoma. Experimental eye research *93*, 528-533.

Linden, J. (2001). Molecular approach to adenosine receptors: receptor-mediated mechanisms of tissue protection. Annual review of pharmacology and toxicology *41*, 775-787.

Liou, G.I., Auchampach, J.A., Hillard, C.J., Zhu, G., Yousufzai, B., Mian, S., Khan, S., and Khalifa, Y. (2008). Mediation of cannabidiol anti-inflammation in the retina by equilibrative nucleoside transporter and A2A adenosine receptor. Invest Ophthalmol Vis Sci *49*, 5526-5531.

Liu, Q., Ju, W.K., Crowston, J.G., Xie, F., Perry, G., Smith, M.A., Lindsey, J.D., and Weinreb, R.N. (2007). Oxidative stress is an early event in hydrostatic pressure induced retinal ganglion cell damage. Invest Ophthalmol Vis Sci *48*, 4580-4589.

Madeira, M., Elvas, F., Martins, J., Ambrósio, A.F., and Santiago, A.R. (2012). Adenosine A2AR blockade prevents retinal microglial activation. Poster Presentation. Paper presented at: 22nd IUBMB & 37th FEBS Congress FEBS Journal (Seville, Spain: Blackwell Publishing Ltd).

Newman, E., and Reichenbach, A. (1996). The Muller cell: a functional element of the retina. Trends in neurosciences *19*, 307-312.

Nimmerjahn, A., Kirchhoff, F., and Helmchen, F. (2005). Resting microglial cells are highly dynamic surveillants of brain parenchyma in vivo. Science *308*, 1314-1318.

Orr, A.G., Orr, A.L., Li, X.J., Gross, R.E., and Traynelis, S.F. (2009). Adenosine A(2A) receptor mediates microglial process retraction. Nature neuroscience *12*, 872-878.

Pan, X.D., Zhu, Y.G., Lin, N., Zhang, J., Ye, Q.Y., Huang, H.P., and Chen, X.C. (2011). Microglial phagocytosis induced by fibrillar beta-amyloid is attenuated by oligomeric beta-amyloid: implications for Alzheimer's disease. Molecular neurodegeneration *6*, 45.

Pekny, M., Wilhelmsson, U., and Pekna, M. (2014). The dual role of astrocyte activation and reactive gliosis. Neuroscience letters *565*, 30-38.

Perigolo-Vicente, R., Ritt, K., Pereira, M.R., Torres, P.M., Paes-de-Carvalho, R., and Giestal-de-Araujo, E. (2013). IL-6 treatment increases the survival of retinal ganglion cells in vitro: the role of adenosine A1 receptor. Biochemical and biophysical research communications *430*, 512-518.

Petersen, M.A., and Dailey, M.E. (2004). Diverse microglial motility behaviors during clearance of dead cells in hippocampal slices. Glia *46*, 195-206.

Pinto-Duarte, A., Coelho, J.E., Cunha, R.A., Ribeiro, J.A., and Sebastiao, A.M. (2005). Adenosine A2A receptors control the extracellular levels of adenosine through modulation of nucleoside transporters activity in the rat hippocampus. J Neurochem *93*, 595-604.

Pournaras, C.J., Rungger-Brandle, E., Riva, C.E., Hardarson, S.H., and Stefansson, E. (2008). Regulation of retinal blood flow in health and disease. Progress in retinal and eye research *27*, 284-330.

Purves, D., Augustine, G.J., Fitzpatrick, D., Katz, L.C., LaMantia, A.-S., McNamara, J.O., and, and Williams, S.M. (2004). Neuroscience, 3rd edition.

Quigley, H.A. (1999). Neuronal death in glaucoma. Progress in retinal and eye research *18*, 39-57.

Quigley, H.A., and Broman, A.T. (2006). The number of people with glaucoma worldwide in 2010 and 2020. The British journal of ophthalmology *90*, 262-267.

Rebola, N., Simoes, A.P., Canas, P.M., Tome, A.R., Andrade, G.M., Barry, C.E., Agostinho, P.M., Lynch, M.A., and Cunha, R.A. (2011). Adenosine A2A receptors control neuroinflammation and consequent hippocampal neuronal dysfunction. J Neurochem *117*, 100-111.

Reigada, D., Lu, W., Zhang, M., and Mitchell, C.H. (2008). Elevated pressure triggers a physiological release of ATP from the retina: Possible role for pannexin hemichannels. Neuroscience *157*, 396-404.

Resta, V., Novelli, E., Vozzi, G., Scarpa, C., Caleo, M., Ahluwalia, A., Solini, A., Santini, E., Parisi, V., Di Virgilio, F., *et al.* (2007). Acute retinal ganglion cell injury caused by intraocular pressure spikes is mediated by endogenous extracellular ATP. The European journal of neuroscience *25*, 2741-2754.

Rungger-Brandle, E., Dosso, A.A., and Leuenberger, P.M. (2000). Glial reactivity, an early feature of diabetic retinopathy. Invest Ophthalmol Vis Sci *41*, 1971-1980.

Salic, A., and Mitchison, T.J. (2008). A chemical method for fast and sensitive detection of DNA synthesis in vivo. Proc Natl Acad Sci U S A *105*, 2415-2420.

Santiago, A.R., Pereira, T.S., Garrido, M.J., Cristovao, A.J., Santos, P.F., and Ambrosio, A.F. (2006). High glucose and diabetes increase the release of [3H]-D-aspartate in retinal cell cultures and in rat retinas. Neurochem Int *48*, 453-458.

Sappington, R.M., Chan, M., and Calkins, D.J. (2006). Interleukin-6 protects retinal ganglion cells from pressure-induced death. Invest Ophthalmol Vis Sci *47*, 2932-2942.

Sappington, R.M., Sidorova, T., Long, D.J., and Calkins, D.J. (2009). TRPV1: contribution to retinal ganglion cell apoptosis and increased intracellular Ca2+ with exposure to hydrostatic pressure. Invest Ophthalmol Vis Sci *50*, 717-728.

Schulte, G., and Fredholm, B.B. (2003). Signalling from adenosine receptors to mitogen-activated protein kinases. Cellular signalling *15*, 813-827.

Selles-Navarro, I., Villegas-Perez, M.P., Salvador-Silva, M., Ruiz-Gomez, J.M., and Vidal-Sanz, M. (1996). Retinal ganglion cell death after different transient periods of pressure-induced ischemia and survival intervals. A quantitative in vivo study. Invest Ophthalmol Vis Sci *37*, 2002-2014.

Siddiqui, T.A., Lively, S., Vincent, C., and Schlichter, L.C. (2012). Regulation of podosome formation, microglial migration and invasion by Ca(2+)-signaling molecules expressed in podosomes. J Neuroinflammation *9*, 250.

Sitkovsky, M.V., and Ohta, A. (2005). The 'danger' sensors that STOP the immune response: the A2 adenosine receptors? Trends in immunology *26*, 299-304.

Streit, W.J. (2000). Microglial response to brain injury: a brief synopsis. Toxicologic pathology *28*, 28-30.

Tezel, G. (2011). The immune response in glaucoma: a perspective on the roles of oxidative stress. Experimental eye research *93*, 178-186.

Tezel, G., and Wax, M.B. (2000). Increased production of tumor necrosis factor-alpha by glial cells exposed to simulated ischemia or elevated hydrostatic pressure induces apoptosis in cocultured retinal ganglion cells. J Neurosci *20*, 8693-8700.

Tezel, G., Yang, X., Luo, C., Peng, Y., Sun, S.L., and Sun, D. (2007). Mechanisms of immune system activation in glaucoma: oxidative stress-stimulated antigen presentation by the retina and optic nerve head glia. Invest Ophthalmol Vis Sci *48*, 705-714.

Trincavelli, M.L., Daniele, S., and Martini, C. (2010). Adenosine receptors: what we know and what we are learning. Current topics in medicinal chemistry *10*, 860-877.

Urcola, J.H., Hernandez, M., and Vecino, E. (2006). Three experimental glaucoma models in rats: comparison of the effects of intraocular pressure elevation on retinal ganglion cell size and death. Experimental eye research *83*, 429-437.

Vindeirinho, J., Costa, G.N., Correia, M.B., Cavadas, C., and Santos, P.F. (2013). Effect of diabetes/hyperglycemia on the rat retinal adenosinergic system. PLoS ONE *8*, e67499.

Vohra, R., Tsai, J.C., and Kolko, M. (2013). The role of inflammation in the pathogenesis of glaucoma. Survey of ophthalmology *58*, 311-320.

Wake, H., Moorhouse, A.J., Jinno, S., Kohsaka, S., and Nabekura, J. (2009). Resting microglia directly monitor the functional state of synapses in vivo and determine the fate of ischemic terminals. J Neurosci *29*, 3974-3980.

Wassle, H. (2004). Parallel processing in the mammalian retina. Nature reviews Neuroscience *5*, 747-757.

Wittendorp, M.C., Boddeke, H.W., and Biber, K. (2004). Adenosine A3 receptor-induced CCL2 synthesis in cultured mouse astrocytes. Glia *46*, 410-418.

Yuskaitis, C.J., and Jope, R.S. (2009). Glycogen synthase kinase-3 regulates microglial migration, inflammation, and inflammation-induced neurotoxicity. Cellular signalling *21*, 264-273.

Zeiss, C.J. (2013). Translational models of ocular disease. Veterinary ophthalmology *16 Suppl 1*, 15-33.

Zeng, X.X., Ng, Y.K., and Ling, E.A. (2000). Neuronal and microglial response in the retina of streptozotocin-induced diabetic rats. Visual neuroscience *17*, 463-471.

Zhang, X., Li, A., Ge, J., Reigada, D., Laties, A.M., and Mitchell, C.H. (2007). Acute increase of intraocular pressure releases ATP into the anterior chamber. Experimental eye research *85*, 637-643.

Zhong, Y., Yang, Z., Huang, W.C., and Luo, X. (2013). Adenosine, adenosine receptors and glaucoma: an updated overview. Biochim Biophys Acta *1830*, 2882-2890.